Electronic Supplementary Material (ESI) for Dalton Transactions.

Cyanoferrocenes as redox-active metalloligands for coordination-driven self-assembly

Luke A. Wilkinson,[a] Thomas T. C. Yue,[a] Emma Massey,[a] Andrew J. P. White[a] and Nicholas J. Long*[a]

Molecular Sciences Research Hub, Imperial College London, White City, London, W12 0BZ

Email: n.long@imperial.ac.uk

Contents:

Experimental

Materials and Methods

All reactions were performed without the need for anerobic techniques. All solvents and most reagents were obtained commercially and used as received. $Cu(MeCN)_4PF_6$ was synthesised using a previously reported procedure, stored in the glovebox but used without further precautions against air.[S1] NMR spectra were recorded on a Bruker Avance 400 MHz spectrometer and referenced to residual solvent peaks of $CDCl_3$ (7.26 ppm), CD_2Cl_2 (5.32 ppm) and acetone-d_6 (2.05 ppm) coupling constants (J) are measured in Hertz (s^{-1}). Mass spectrometry analyses were conducted by Lisa Haigh of the mass spectrometry service at Imperial College London and microanalyses were carried out by Stephen Boyer at London Metropolitan University with use of a Thermo Scientific (Carlo Erba) Flash 2000 Organic Elemental Analyser, configured for %CHN. Voltammetry experiments (cyclic, differential pulse and square wave) were recorded on a Gamry reference 600™ (Gamry Instruments, Warminter, PA, USA) under an atmosphere of dry N_2 gas in a solution of CH_2Cl_2 with 0.1 M $N^nBu_4PF_6$. A standard 3-electrode setup was employed consisting of a 3 mm glassy carbon working electrode and two separate Pt wires for reference and auxillary electrodes. All potentials are referenced to the Fc/Fc^+ redox couple and corrected for resistance. All computational calculations were carried out using the B3LYP functional and the 6-311+G (d,p) basis set, as implemented in Gaussian 09. Structural optimisations were carried out under no symmetry constraints.

Synthesis

Comments on the synthesis and purification of formylferrocenes

The syntheses of 1,1'-[S2,S3] and 1,2-diformylferrocenes[S4] were achieved according to the literature procedures, however, their purification has been modified. In our hands, after evaporation of the product fraction from the column, a persistent, sticky, dark-red oil remains which cannot be converted into a solid by washing with water (to remove excess DMF) or by placing under a high vacuum for an extended period of time. As an oil, the product readily decomposes to form a dark brown coating on the glassware that is no longer soluble in Et_2O. This issue is easily overcome by the addition and subsequent evaporation of diethyl ether and/or hexane. Multiple iterations of this procedure can generate the stable bright-red powder described in the literature. Occasionally, the powder may be accompanied by a lighter (orange) oil, but this can be removed by trituration with hexane to yield the red powder cleanly. This procedure appears to be general to all formylferrocenes that we have employed.

Yield of 1,1'-diformylferrocene was 86 % and 1,2-diformylferrocene was 76 %

Optimisation of procedure for conversion of formylferrocenes to cyanoferrocenes

The reagents (1,2'-Fc(CHO)$_2$ and I$_2$) were dissolved in THF, then added to aqueous ammonia and the reaction was stirred. To quench the reaction, a saturated aqueous solution of sodium thiosulfate is added into the reaction.

When optimising reaction timescale, a 1 mL aliquot from the reaction was removed at defined timepoints and added straight into the aforementioned sodium thiosulfate solution. The organic products were extracted with Et$_2$O and dried over MgSO$_4$ before evaporation. The ^{1}H NMR spectrum of this solid was obtained and the integrals of starting material and product were compared to generate % conversions.

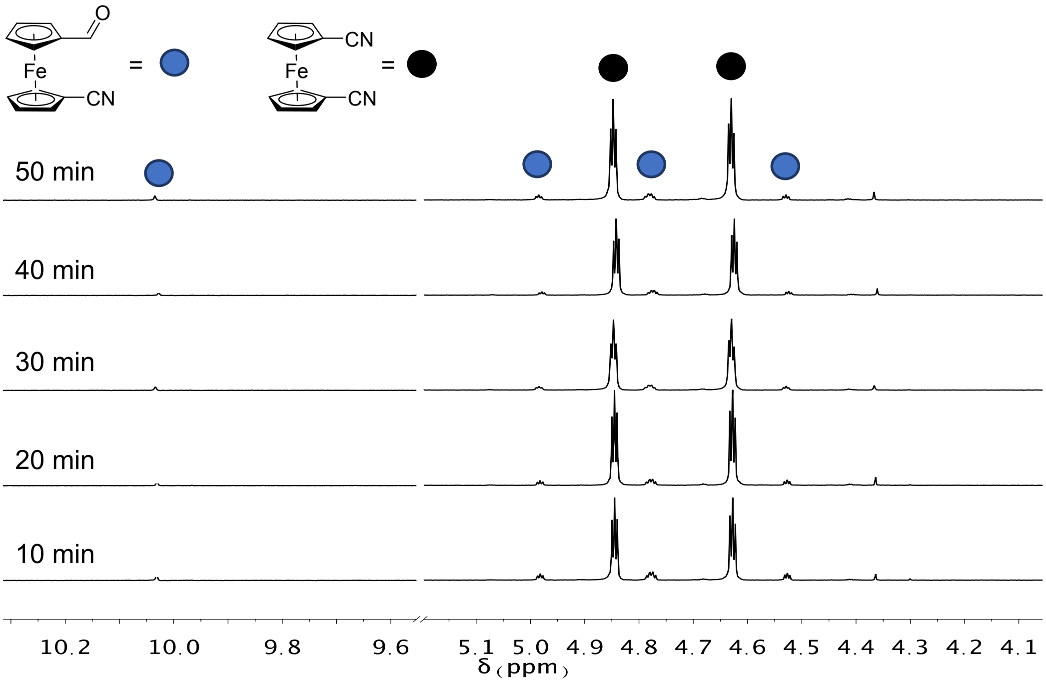

Figure S1: Following the reaction progress over time by ^{1}H NMR spectroscopy in CDCl$_3$ (400 MHz). Only the relevant areas of the spectrum are shown for clarity. No reaction progress after 10 minutes.

To determine the optimum quantity of I_2 needed, the reaction was undertaken as described in the optimised procedure but the number of equivalents of I_2 was varied. After the reaction was complete, the crude reaction mixture was extracted into Et_2O, dried over $MgSO_4$ and evacuated to dryness. The ^1H NMR spectrum was then obtained in $CDCl_3$.

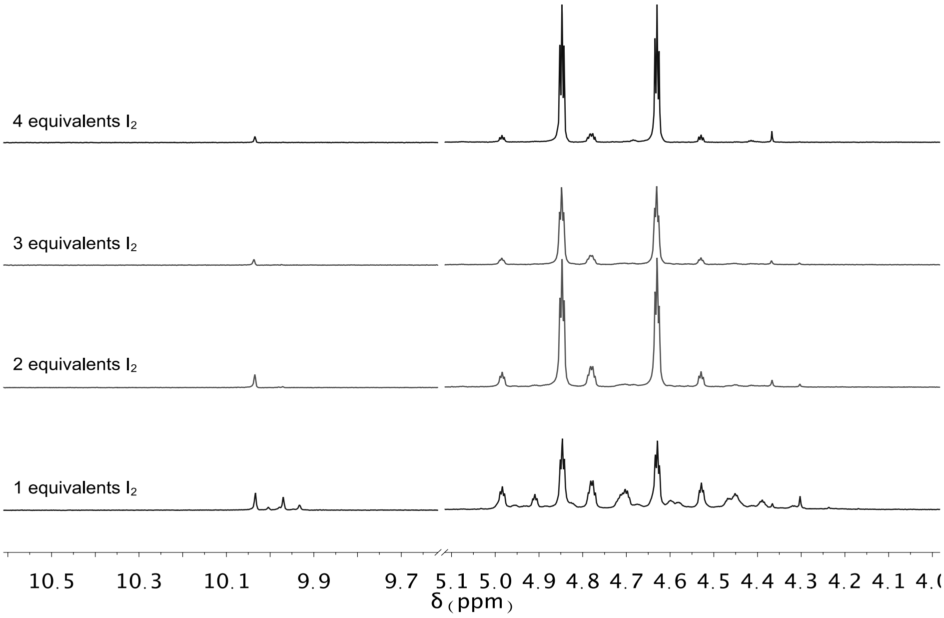

Figure S2: ^1H NMR spectra in $CDCl_3$ (400 MHz) showing the effect of I_2 concentration on the reaction progress.

General Optimised Procedure for the synthesis of cyanoferrocenes from formylferrocenes

Ammonium hydroxide solution (50 mL, 35% NH_3 in H_2O) was added to a solution of formylferrocene (1 equivalent) and iodine (1 equivalent per aldehyde) in tetrahydrofuran (ca. 10-25 mL, *i.e.* enough to dissolve the reagents). The reaction mixture was then stirred in a sealed vessel for 10 min in the dark at room temperature, before quenching with saturated aqueous $Na_2S_2O_3$ solution. The organic layer was then extracted into diethyl ether (2 × 20 mL) and dried over $MgSO_4$. All volatiles were removed *in vacuo* and the subsequent dark orange solid was purified by flash chromatography (SiO_2, Et_2O). The first (yellow) band was isolated as a light orange powder which was passed through a silica plug (CH_2Cl_2) and evacuated to yield the desired product as a bright yellow solid.

Cyanoferrocene

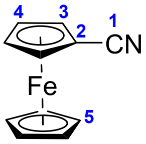

From 1.00 g (4.7 mmol) of ferrocenecarboxaldehyde and 1.19 g, (4.7 mmol) of iodine, obtained 0.86 g, 4.1 mmol (87 %). ^{1}H NMR (400 MHz, 298 K) ***$CDCl_3$*** **δ_H**: 4.68 (pseudo- t, $^3J_{\alpha,\beta}$ 1.8 Hz, 2H, *H*4), 4.41 (pseudo- t, $^3J_{\alpha,\beta}$ 1.8 Hz, 4H, *H*3), 4.37 (s, 5H, *H*5); ^{13}C (100 MHz, $CDCl_3$) **δ_C**: 120.0 (*C*1), 71.7 (*C*2), 70.7 (*C*4), 70.6 (*C*5), 51.9 (*C*2). **IR** (ATR, *v* (cm^{-1} 2225 (m, CN); **HRMS** m/z (ES-TOF, +ve): *Calc.* for $C_{11}H_9NFe$, 211.0084 Found, 211.0088 **Elemental Analysis**: *Calc.* C 62.60, H 4.30, N 6.64. *Found* C 62.46, H 4,39, N 6.57.

1,1'-Dicyanoferrocene

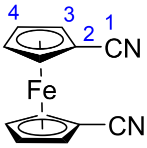

From 0.1 g (0.41 mmol) of 1,1'-ferrocenedicarboxaldehyde and 0.21 g, (0.82 mmol) of iodine , obtained 0.088 g, 4.1 mmol (91 %).^{1}H NMR (400 MHz, 298 K) ***$CDCl_3$***: **δ_H** 4.82 (t, $^3J_{HH}$ = 2.0 Hz, 4H, *H*4), 4.63 (t, $^3J_{HH}$ = 2.0 Hz, 4H, *H*3); ^{13}C NMR (100 MHz, 298 K): **δ_C** 118.3 (*C*1), 73.9 (*C*3), 73.6 (*C*4), 54.8 (*C*2); ^{1}H NMR (400 MHz, 298 K) ***$(CD_3)_2CO$***: **δ_H** 4.98 (t, $^3J_{HH}$ = 2.0 Hz, 4H, Cp *H*), 4.73 (t, $^3J_{HH}$ = 2.0 Hz, 4H, Cp *H*) **IR** (ATR, *v*(cm^{-1})): 2225 (m, CN); **HRMS** m/z (ES-TOF, +ve): calcd for $C_{12}H_8FeN_2$, 236.0037; found, 236.0047. **Elemental Analysis**: *Calc.* C 61.06, H 3.42, N 11.87 *Found*. C 60.94, H 3.51, N 11.75

1,2-Dicyanoferrocene

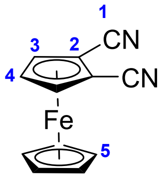

From 0.22 g (0.9 mmol) of 1,2-ferrocenedicarboxaldehyde and 0.45 g, (1.8 mmol) of iodine, obtained 0.184 g, 0.78 mmol (87 %). ^{1}H NMR (400 MHz, 298 K) ***$CDCl_3$***: **δ_H** 4.89 (d, $^3J_{HH}$ = 2.7 Hz, 2H, *H*3), 4.64 (t, $^3J_{HH}$ = 2.8 Hz, 1H, *H*4), 4.57 (s, 5H, *H*5); ^{13}C NMR (100 MHz, 298 K): **δ_C** 118.3 (*C*1), 73.9 (*C*3), 73.6 (C*4*), 65.8 (*C*5), 56.0 (*C*2); ^{1}H NMR (400 MHz, 298 K) ***CD_2Cl_2***: **δ_H** 4.95 (d, $^3J_{HH}$ = 2.7 Hz, 2H, *H*3), 4.70 (t, $^3J_{HH}$ = 2.8 Hz, 1H, *H*4), 4.59 (s, 5H, *H*5); ^{13}C NMR (100 MHz, 298 K): **δ_C** 116.7 (*C*1), 74.4 (*C*3), 73.4 (C*4*), 72.9 (*C*5), 55.9 (*C*2); ^{1}H NMR (400 MHz, 298 K) ***$(CD_3)_2CO$***: **δ_H** 5.07 (d, $^3J_{HH}$ = 2.7 Hz, 2H, *H*3), 4.80 (t, $^3J_{HH}$ = 2.8 Hz, 1H, *H*4), 4.59 (s, 5H, *H*5); **IR** (ATR, *v*(cm^{-1})): 2225 (m, CN); **HRMS** m/z (ES-TOF, +ve): *Calc*. for $C_{12}H_8FeN_2$, 236.0037; *Found*, 236.0034. **Elemental Analysis**: *Calc*. C 61.06, H 3.42, N 11.87 *Found*. C 60.96, H 3.44, N 11.69

$[Cu(1,2\text{-}Fc(CN)_2)_2]_\infty[PF_6]_\infty$ (**1**)

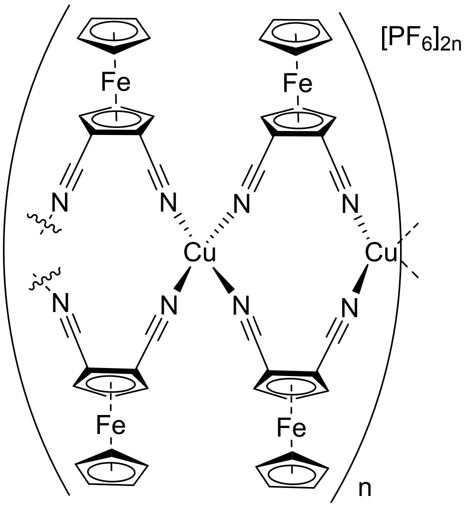

$[Cu(NCMe)_4][PF_6]$ (6.5 mg, 17 µmol) was dissolved in THF (2 mL). 1,2-Fc$(CN)_2$ (4.1 mg, 17 µmol) was dissolved in CH_2Cl_2 (2 mL) and added dropwise to the solution of $[Cu(NCMe)_4][PF_6]$. The reaction was stirred for 30 mins, during which time, a light orange precipitate was generated. The precipitate was washed with CH_2Cl_2 and evacuated to dryness to yield **1** (5.1 mg, 7.5 µmol, 43 %). Crystals of suitable quality for X-ray crystallography measurements were obtained from the slow diffusion of a THF solution of $[Cu(NCMe)_4][PF_6]$ into a CH_2Cl_2 solution of 1,2-Fc$(CN)_2$.

IR (ATR, *v*(cm^{-1})): 2239 (m, CN), 2250 (m, CN) **Elemental Analysis**: for $C_{24}H_{16}CuF_6Fe_2N_4P$ *Calc*. C 42.35, H 2.37, N 8.23 *Found*. C 42.45, H 2.12, N 8.55

$[(PPh_3)_2Cu]_2[\mu\text{-}1,2\text{-}Fc(CN)_2]_2(PF_6)_2$ (**2**)

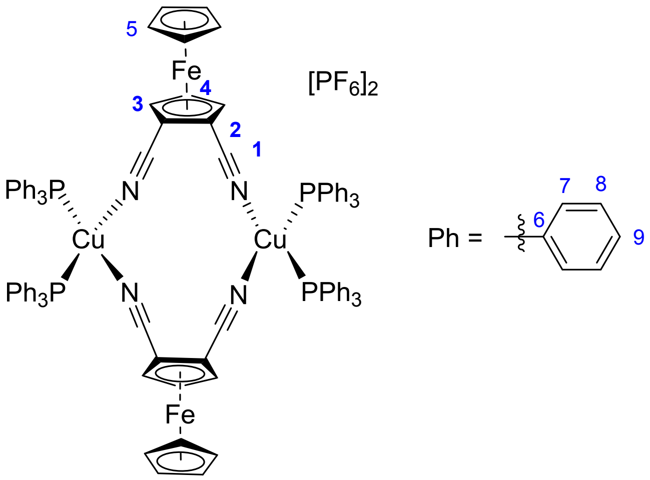

$Cu(NCMe)_4PF_6$ (0.08 g, 0.21 mmol) and PPh_3 (0.112 g, 0.43 mmol) were stirred in MeCN (2 mL) for 10 minutes and then evacuated to dryness. The resulting complex was re-dissolved in THF (2 mL) and a solution of 1,2-$Fc(CN)_2$ (0.1 g, 0.42 mmol) in CH_2Cl_2 (2 mL) was added dropwise. The reaction was stirred for 30 mins, during which time, a light orange precipitate (**2**) was generated. The excess solvent was decanted off to yield a solid which was evacuated to dryness. Obtained 0.186 g, 0.096 mmol, 91 % Crystals of suitable quality for X-ray crystallography measurements were obtained from the slow diffusion of hexane into a THF solution of **2**.

^1H NMR (400 MHz, 298 K) ***CD_2Cl_2***: **δ_H** 7.6-6.9 (br 60H, *H7-9*) 5.05 (d, $^3J_{HH}$ = 2.8 Hz, 2H, *H*3), 4.90 (t, $^3J_{HH}$ = 2.8 Hz, 1H, *H*4), 4.45 (s, 5H, *H*5), ^{13}C NMR (100 MHz, 298 K): **δ_C** 133.4, 131.1, 129.3 (*C7*-9), 73.9 (*C*5); $^{31}P\{^1H\}$ NMR (162 MHz, 298 K): **δ_P** 0.7 (br, *P*Ph_3), -144.4 (septet, $^1J_{PF}$ = 710 Hz, *P*F_6); ^1H NMR (400 MHz, 298 K) **(*$CD_3)_2CO$*: δ_H** 7.59-7.34 (m, 60H, *H*7-9), 5.19 (d, $^3J_{HH}$ = 2.8 Hz, 4H, *H*3), 4.91 (t, $^3J_{HH}$ = 2.8 Hz, 2H, *H*4), 4.59 (s, 5H, *H*5); **IR** (ATR, *v*(cm^{-1})): 2230, 2239 (m, CN); **Elemental Analysis**: for $C_{96}H_{76}Cu_2F_{12}Fe_2N_4P_6.CH_2Cl_2$ *Calc*. C 57.58, H 3.89, N 2.77 *Found*. C 57.11, H 3.13, N 2.77

$[(dppf)Cu]_2[\mu\text{-}1,2\text{-}Fc(CN)_2]_2(PF_6)_2$ (**3**)

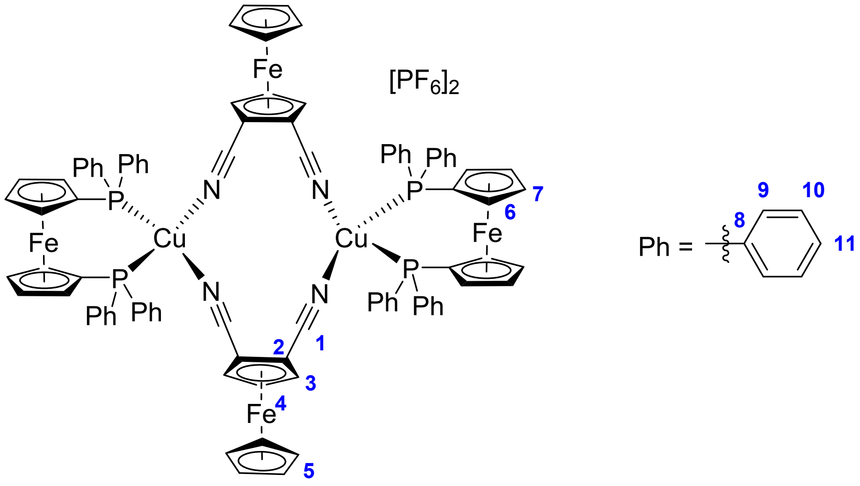

$Cu(NCMe)_4PF_6$ (0.04 g, 0.105 mmol) and 1,1'-bisdiphenylphosphinoferrocene (dppf) (0.06 g, 0.105 mmol) were stirred in MeCN (2 mL) for 10 minutes and then evacuated to dryness. The resulting complex was re-dissolved in THF (2 mL) and a solution of 1,2-$Fc(CN)_2$ (0.025 g, 0.105 mmol) in CH_2Cl_2 (2 mL) was added dropwise. The reaction was stirred for 30 mins, during which time, a light orange precipitate (**2**) was generated. The excess solvent was decanted off to yield a solid which was washed with Et_2O and evacuated to dryness. Obtained 0.084 g, 0.042 mmol, 53 %

^{1}H NMR (400 MHz, 298 K) ***$(CD_3)_2CO$***: $\boldsymbol{\delta_H}$ 7.67-7.46 (m, 20H, *H*8-11), 5.19 (d, $^3J_{HH}$ = 2.8 Hz, 4H, *H*3), 4.91 (t, $^3J_{HH}$ = 2.8 Hz, 2H, *H*4), 4.61 (s, 10H, *H*5) 4.59 (br, 4H, *H*7), 4.39 (br, 4H, *H*6); **IR**: (ATR, *v*(cm^{-1})): 2230, 2241 (m, CN) **HRMS** m/z (ES-TOF, +ve): calcd for $C_{46}H_{36}N_2P_2CuFe_2$, 853.0349; found, 853.0363 (M^+). **Elemental Analysis**: for $C_{92}H_{72}CuF_{12}Fe_4N_4P_2$ *Calc*. C 55.31, H 3.63, N 2.80 *Found*. C 55.43, H 3.55, N 2.92

[(dppf)Cu]$_2$(μ-dppf)(PF$_6$) (**4**)

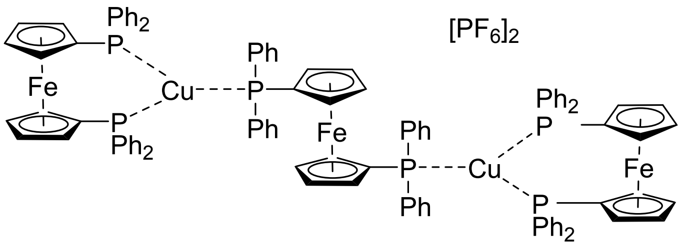

Crystals of **4** were obtained by layering a THF solution of [Cu(dppf)(NCMe)$_2$][PF$_6$] with a Et$_2$O solution of 1,2-Fc(CN)$_2$. Obtained a small unmeasured quantity of orange block crystals.

^{1}H NMR (400 MHz, 298 K, ***CD$_2$Cl$_2$***): **δ_H** 7.6-6.9 (br 60H, *H7-9*) 5.05 (d, $^3J_{HH}$ = 2.8 Hz, 2H, *H*3), 4.90 (t, $^3J_{HH}$ = 2.8 Hz, 1H, *H*4), 4.45 (s, 5H, *H*5), ^{13}C NMR (100 MHz, 298 K): **δ_C** 133.4, 131.1, 129.3 (*C7*-9), 73.9 (*C*5); ^{31}P{^{1}H} NMR (162 MHz, 298 K): **δ_P** -9.4 (br, dppf) -144.3 (septet, $^1J_{PF}$ = 707 Hz, *P*F$_6$); **Elemental Analysis**: for $C_{102}H_{84}Cu_2F_{12}Fe_3P_8$ *Calc*. C 58.63, H 4.07 *Found*. C 58.63, H 4.16

$[(PPh_3)_2Cu][\mu\text{-}1,1'\text{-}Fc(CN)_2]_\infty(PF_6)_\infty$ (**5**)

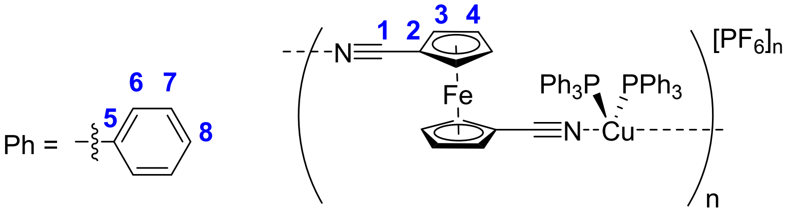

$Cu(NCMe)_4PF_6$ (0.08 g, 0.21 mmol) and PPh_3 (0.11 g, 0.43 mmol) were stirred in MeCN (2 mL) for 2 hours and then evacuated to dryness. The resulting complex was re-dissolved in THF (2 mL) and a solution of 1,2-$Fc(CN)_2$ (0.10 g, 0.42 mmol) in CH_2Cl_2 (2 mL) was added dropwise. The reaction was stirred for 30 mins and then Et_2O (7.5 mL) was added to afford a light orange precipitate. The excess solvent was decanted off to yield a solid which was evacuated to dryness. Obtained 0.094 g, 0.048 mmol, 46 %. Crystals of suitable quality for X-ray crystallography measurements were obtained from slow evaporation of chloroform.

^{1}H NMR (400 MHz, 298 K) ***$CDCl_3$***: **δ_H** 7.55-7.30 (m, 10 H, *H*6-8) 4.79 (pseudo-t, 4H, *H*3), 4.63 (pseudo-t, 4H, *H*4), ^{13}C NMR (100 MHz, 298 K): **δ_C** 133.5, 130.7, 129.0 (*C*6-8) 118.8 (*C*1), 75.0 (*C*3), 73.9 (*C*4), 54.8 (*C*2), ^{31}P{^{1}H} NMR (162 MHz, 298 K): **δ_P** 0.4 (br, *P*Ph$_3$), -144.4 (septet, $^1J_{PF}$ = 713 Hz, *P*F$_6$); ^{1}H NMR (400 MHz, 298 K) ***CD_2Cl_2***: **δ_H** 7.58-7.30 (m, 10 H, *H*6-8) 4.76 (pseudo-t, , $^3J_{HH}$ = 1.8 Hz, 4H, *H*3), 4.61 (pseudo-t, $^3J_{HH}$ = 1.8 Hz, 4H, *H*4), ^{13}C NMR (100 MHz, 298 K): **δ_C** 133.5, 130.7, 129.0 (*C*6-8) 118.2 (*C*1), 74.5 (*C*3), 73.8 (C*4*), 55.3 (*C*2), ^{31}P{^{1}H} NMR (162 MHz, 298 K): **δ_P** 0.5 (br, *P*Ph$_3$), -144.4 (septet, $^1J_{PF}$ = 710 Hz, *P*F$_6$); **IR** (ATR, *v*(cm^{-1})): 2243 (m, CN); **Elemental Analysis**: for $C_{50}H_{44}CuF_6FeN_2P_3$ *Calc*. C 60.10, H 4.44, N 2.80 *Found*. C 59.37, H 3.82, N 3.05

$[(dppf)Cu][\mu\text{-}1,1'\text{-}Fc(CN)_2]_\infty(PF_6)_\infty$ (**6**)

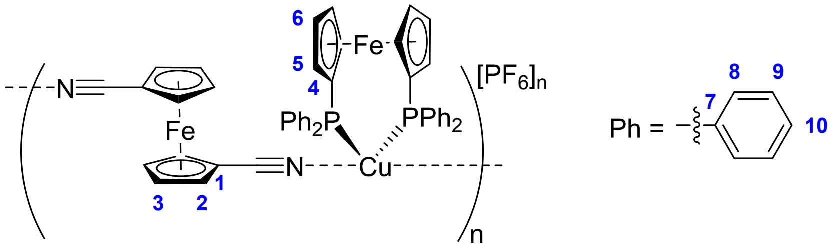

$Cu(NCMe)_4PF_6$ (0.06 g, 0.16 mmol) and 1,1'-bisdiphenylphosphinoferrocene (dppf) (0.09 g, 0.16 mmol) were stirred in MeCN (2 mL) for 18 hours and then evacuated to dryness. The resulting complex was re-dissolved in THF (2 mL) and a solution of 1,2-$Fc(CN)_2$ (0.04 g, 0.16 mmol) in CH_2Cl_2 (10 mL) was added dropwise. The reaction was stirred for 30 mins, during which time, a light orange precipitate (**6**) was generated. The excess solvent was decanted off to yield a solid which was washed with CH_2Cl_2 and Et_2O then evacuated to dryness. Obtained 0.100 g, 0.1 mmol, 62 %

^{1}H NMR (400 MHz, 298 K, ***$(CD_3)_2CO$***): **δ_H** 7.70-7.50 (m, 20H, *H*8-10), 5.01 (pseudo-t, $^3J_{HH}$ = 2.7 Hz, 4H, *H*2), 4.79 (pseudo-t, $^3J_{HH}$ = 2.8 Hz, 4H, *H*3), 4.57 (br, 4H, *H*5), 4.38 (br, 4H, *H*6); **IR** (ATR, *v*(cm^{-1})): 2240 (m, CN); **HRMS** m/z (ES-TOF, +ve): calcd for $C_{46}H_{36}N_2P_2CuFe_2$, 853.0349; found, 853.0361 (M$^+$).

Crystallography

The X-ray crystal structure of 1

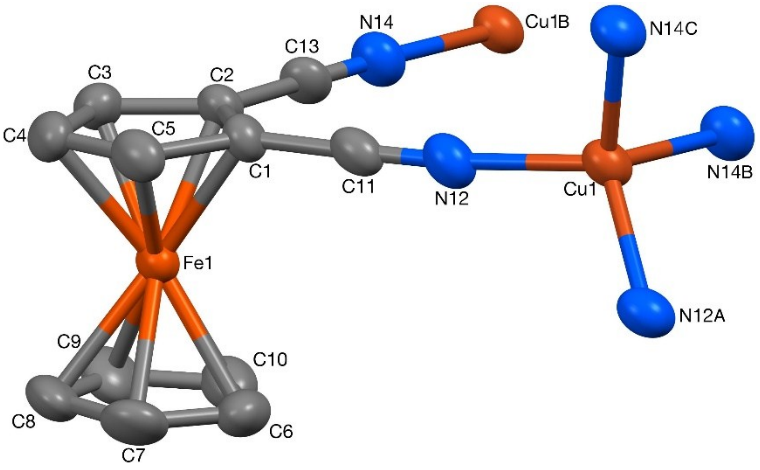

Figure S3: The structure of the unique portion of the cationic polymer chain present in the crystal of **1** showing how it links to adjacent atoms (50% probability ellipsoids).

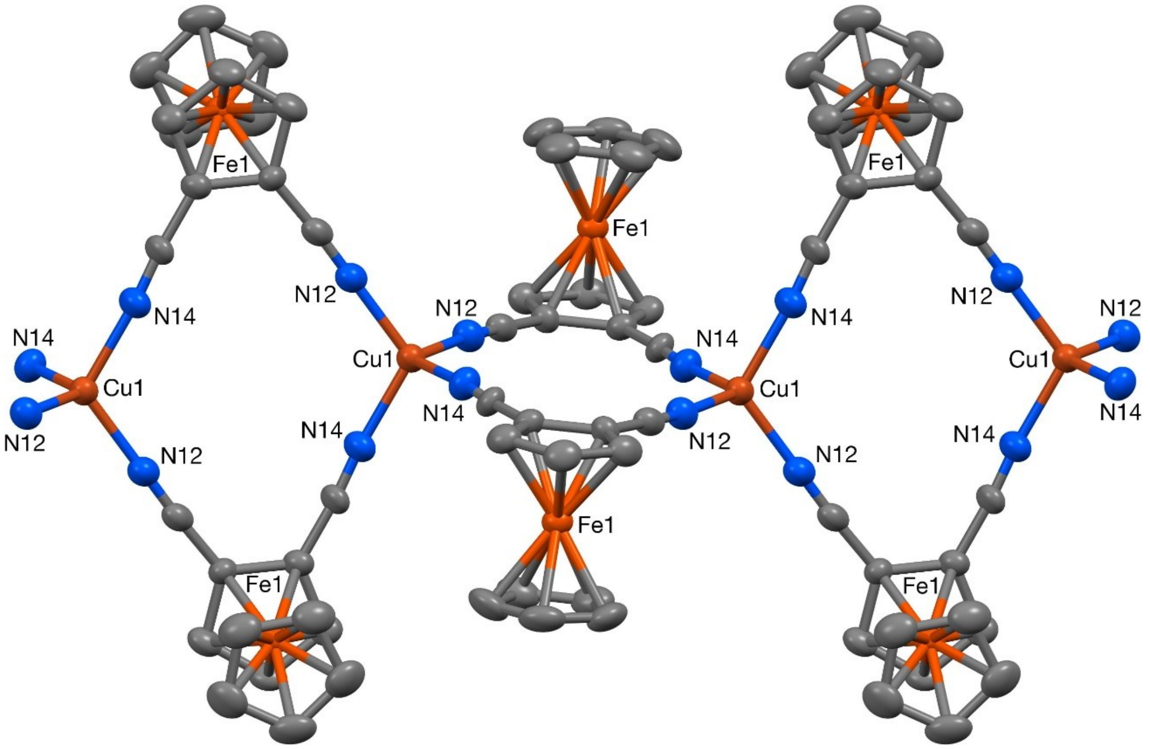

Figure S4: Part of the extended cationic polymer chain present in the structure of **1** (50% probability ellipsoids)

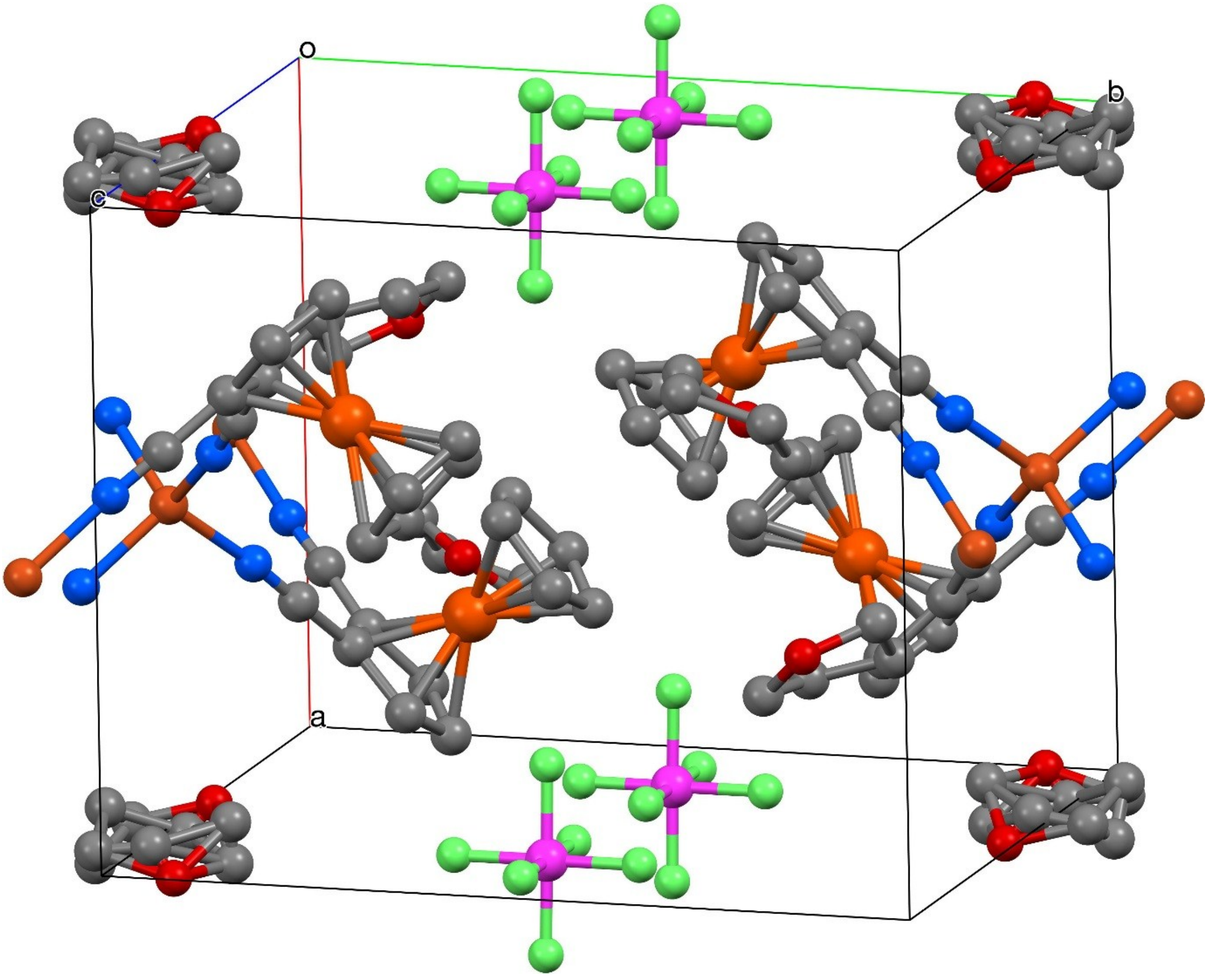

Figure S5*:* The contents of the unit cell in the structure of **1**.

Crystal data for **1**: [$C_{24}H_{16}CuFe_2N_4$](PF_6)·3C_4H_8O, *M* = 896.93, monoclinic, *P*2/*c* (no. 13), *a* = 11.3250(2), *b* = 13.8008(3), *c* = 12.4291(2) Å, β = 92.4850(19)°, *V* = 1940.77(7) Å^3, *Z* = 2 [C_2 symmetry], D_c = 1.535 g cm^{-3}, μ(Cu-Kα) = 7.544 mm^{-1}, *T* = 173 K, orange platy needles, Agilent Xcalibur PX Ultra A diffractometer; 3711 independent measured reflections (R_{int} = 0.0389), F^2 refinement,[X1,X2] R_1(obs) = 0.0500, wR_2(all) = 0.1350, 2708 independent observed absorption-corrected reflections [$|F_o| > 4\sigma(|F_o|)$, completeness to θ_{full}(67.7°) = 98.3%], 281 parameters. CCDC 1873791.

The O30- and O40-based included THF solvent molecules in the structure of **1** were both found to be disordered. For the former, two orientations were identified of *ca*. 66 and 34% occupancy whilst for the latter, which is adjacent to a 2-fold axis, two unique orientations were identified of *ca*. 27 and 23% occupancy (with two further orientations of the same occupancies being generated by operation of the C_2 axis). The geometries of both pairs of orientations were optimised, the thermal parameters of adjacent atoms were restrained to be similar, and only the non-hydrogen atoms of the major occupancy orientation were refined anisotropically (those of the minor occupancy orientations were refined isotropically).

Table S1. Selected bond lengths (Å) and angles (°) for **1**.

Cu(1)–N(12)	1.969(4)	Cu(1)–N(12A)	1.969(4)
Cu(1)–N(14B)	1.989(4)	Cu(1)–N(14C)	1.989(4)
C(11)–N(12)	1.150(6)	C(13)–N(14)	1.124(6)

N(12)–Cu(1)–N(12A)	111.4(2)	N(12)–Cu(1)–N(14B)	115.65(16)
N(12)–Cu(1)–N(14C)	105.21(16)	N(12A)–Cu(1)–N(14B)	105.21(16)
N(12A)–Cu(1)–N(14C)	115.65(16)	N(14B)–Cu(1)–N(14C)	103.8(2)

The X-ray crystal structure of 2

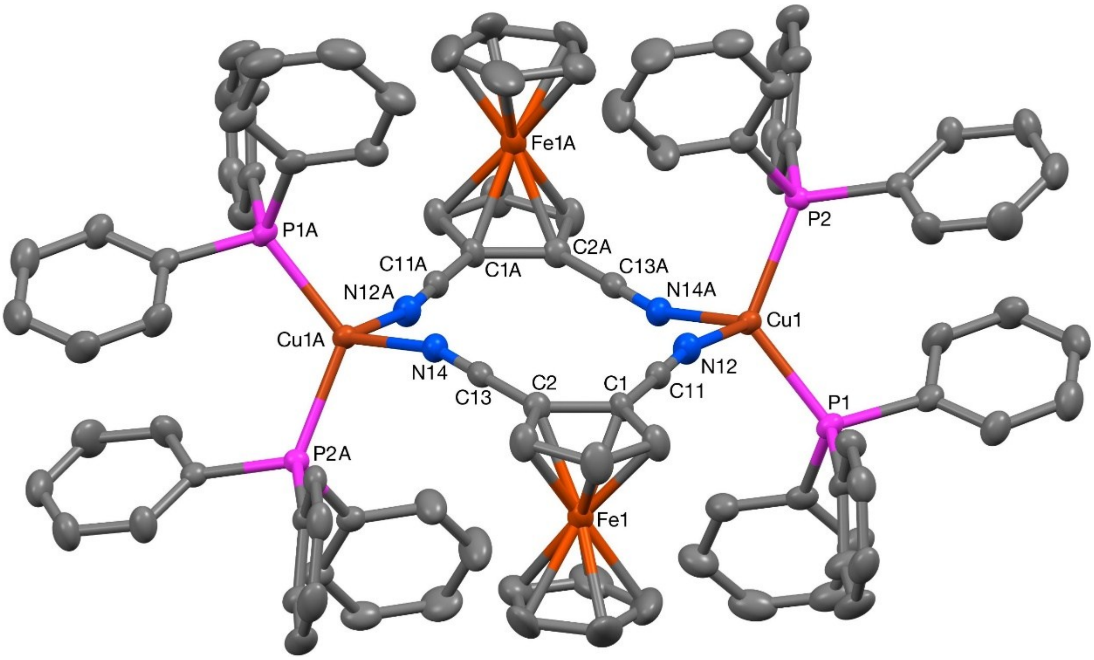

Figure S6: The structure of the di-cation present in the crystal of **2** (50% probability ellipsoids).

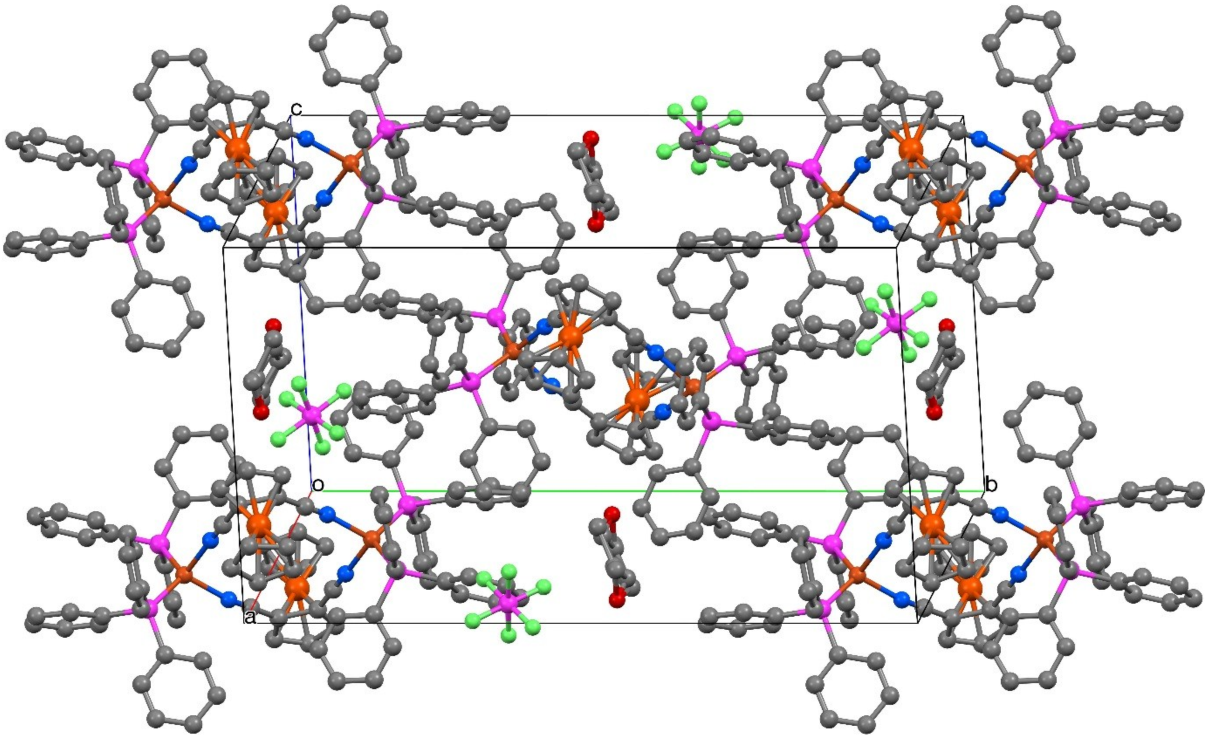

Figure S7: The contents of the unit cell in the structure of **2**.

Crystal data for **2**: $[C_{96}H_{76}Cu_2Fe_2N_4P_4](PF_6)_2 \cdot C_4H_8O$, M = 2010.31, monoclinic, $P2_1/c$ (no. 14), a = 12.7243(3), b = 25.1229(6), c = 14.1878(4) Å, β = 96.972(2)°, V = 4501.9(2) Å^3, Z = 2 [C_i symmetry], D_c = 1.483 g cm^{-3}, μ(Mo-Kα) = 0.965 mm^{-1}, T = 173 K, orange blocks, Agilent Xcalibur 3 E diffractometer; 9045 independent measured reflections (R_{int} = 0.0196), F^2 refinement,[X1,X2] R_1(obs) = 0.0428, wR_2(all) = 0.1021, 7056 independent observed absorption-corrected reflections [$|F_o| > 4\sigma(|F_o|)$, completeness to θ_{full}(25.2°) = 99.3%], 627 parameters. CCDC 1873792.

The C6-based cyclopentadienyl ring, the P60-based hexafluorophosphate anion, and the O70-based included THF solvent molecule in the structure of **2** were all found to be disordered. For both the C6-based cyclopentadienyl ring and the P60-based hexafluorophosphate anion, two orientations were identified, of *ca*. 84:16 and 88:12% occupancy respectively. In each case the geometries of the two orientations were optimised, the thermal parameters of adjacent atoms were restrained to be similar, and only the non-hydrogen atoms of the major occupancy orientations were refined anisotropically (those of the minor occupancy orientations were refined isotropically). The O70-based THF solvent molecule was found to be disordered across an inversion centre, and this was modelled using one unique 50% occupancy orientation (with a second 50% occupancy orientation being generated by operation of the inversion centre). The geometry of the unique orientation was optimised and all of the non-hydrogen atoms were refined anisotropically.

Table S2. Selected bond lengths (Å) and angles (°) for **2**.

Cu(1)–P(1)	2.2655(8)	Cu(1)–P(2)	2.2858(8)
Cu(1)–N(12)	2.040(2)	Cu(1)–N(14A)	2.042(2)
C(11)–N(12)	1.139(4)	C(13)–N(14)	1.141(3)
P(1)–Cu(1)–P(2)	120.57(3)	P(1)–Cu(1)–N(12)	103.23(7)
P(1)–Cu(1)–N(14A)	118.30(7)	P(2)–Cu(1)–N(12)	111.70(8)
P(2)–Cu(1)–N(14A)	102.13(7)	N(12)–Cu(1)–N(14A)	99.01(10)

The X-ray crystal structure of 4

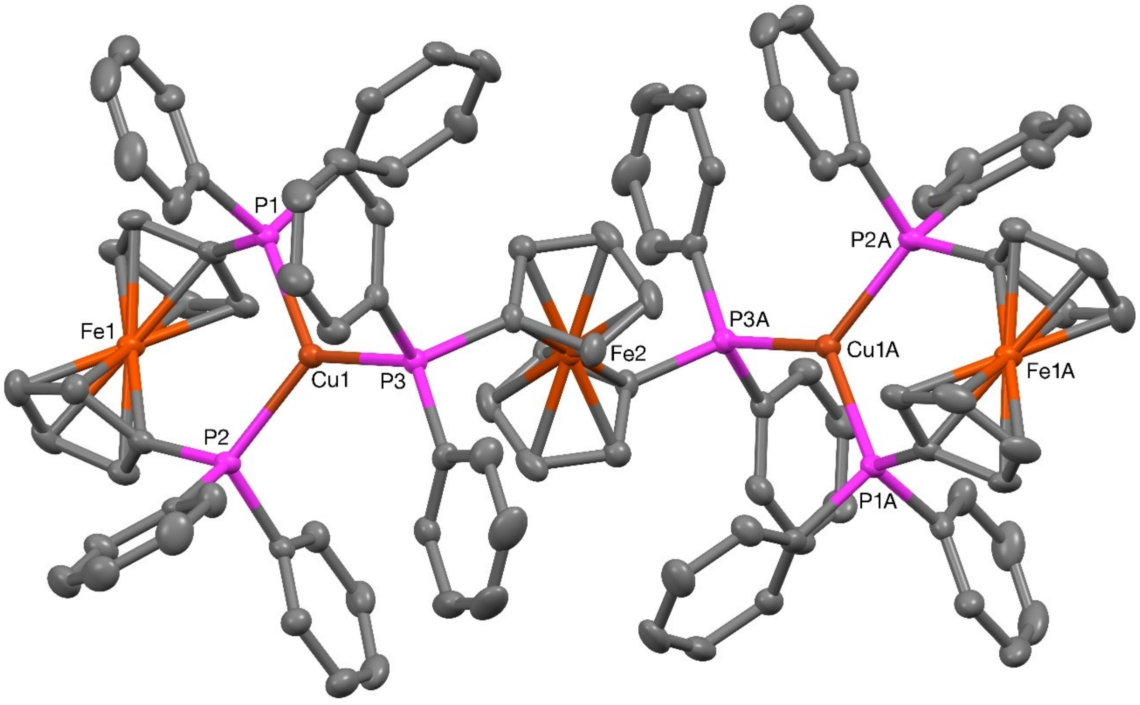

Figure S8: The structure of the di-cation present in the crystal of **4** (50% probability ellipsoids).

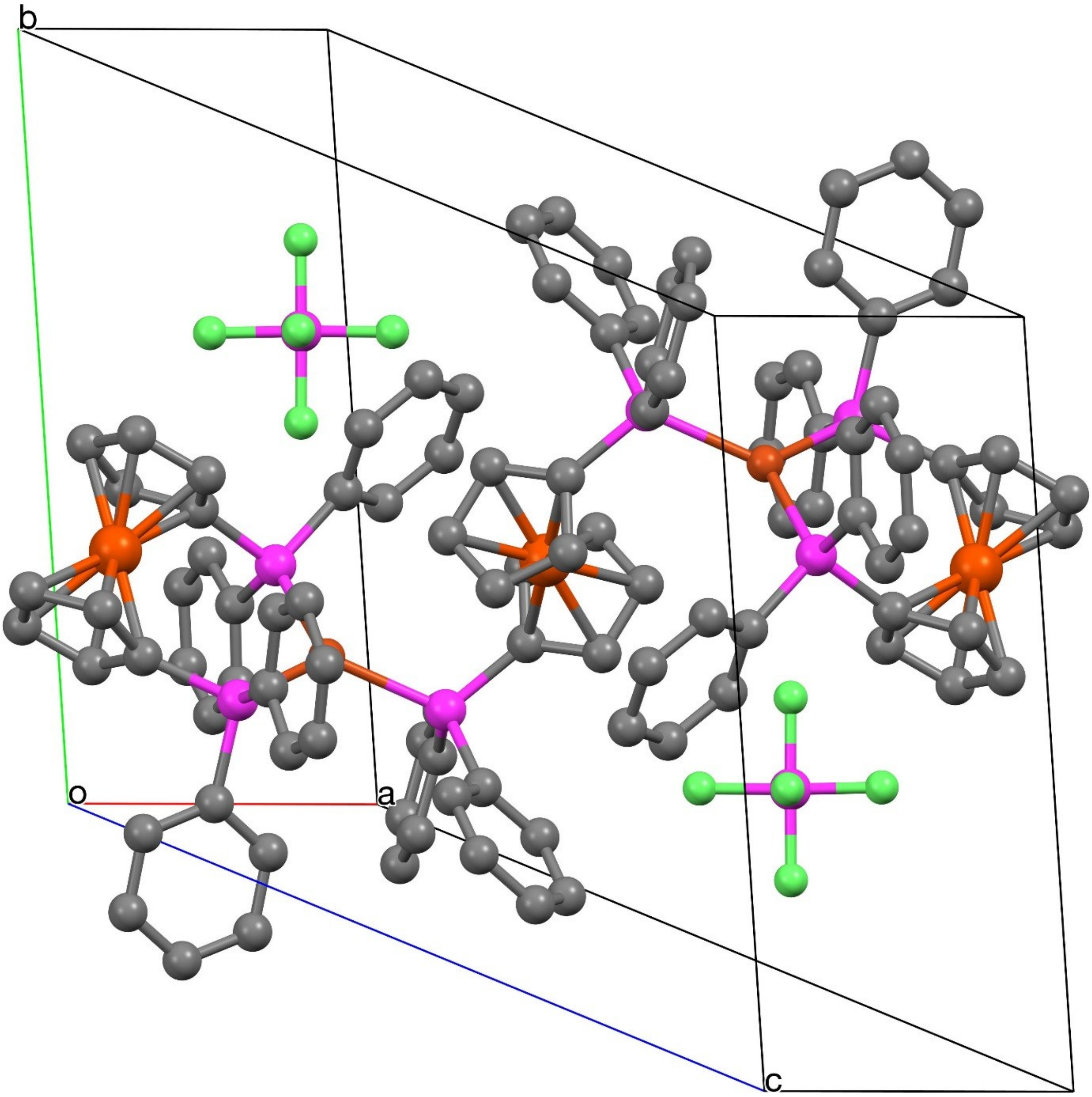

Figure S9: The contents of the unit cell in the structure of **4**.

Crystal data for **4**: $[C_{102}H_{84}Cu_2Fe_3P_6](PF_6)_2$, M = 2080.08, triclinic, P-1 (no. 2), a = 11.1061(5), b = 14.3584(6), c = 15.3808(7) Å, α = 98.506(4), β = 95.158(4), γ = 110.712(4)°, V = 2241.97(18) Å^3, Z = 1 [C_i symmetry], D_c = 1.541 g cm^{-3}, μ(Mo-Kα) = 1.158 mm^{-1}, T = 173 K, orange blocks, Agilent Xcalibur 3 E diffractometer; 8836 independent measured reflections (R_{int} = 0.0200), F^2 refinement,[X1,X2] R_1(obs) = 0.0375, wR_2(all) = 0.0827, 7030 independent observed absorption-corrected reflections [$|F_o| > 4\sigma(|F_o|)$, completeness to θ_{full}(25.2°) = 98.5%], 604 parameters. CCDC 1873793.

The P10-based hexafluorophosphate anion in the structure of **3** was found to be disordered. Two orientations were identified of *ca*. 87 and 13% occupancy, their geometries were optimised, the thermal parameters of adjacent atoms were restrained to be similar, and only the atoms of the major occupancy orientation were refined anisotropically (those of the minor occupancy orientation were refined isotropically).

Table S3. Selected bond lengths (Å) and angles (°) for **4**.

Cu(1)–P(1)	2.2907(7)	Cu(1)–P(2)	2.2693(8)
Cu(1)–P(3)	2.2649(7)		
P(1)–Cu(1)–P(2)	111.59(3)	P(1)–Cu(1)–P(3)	123.43(3)
P(2)–Cu(1)–P(3)	124.37(3)		

The X-ray crystal structure of 5

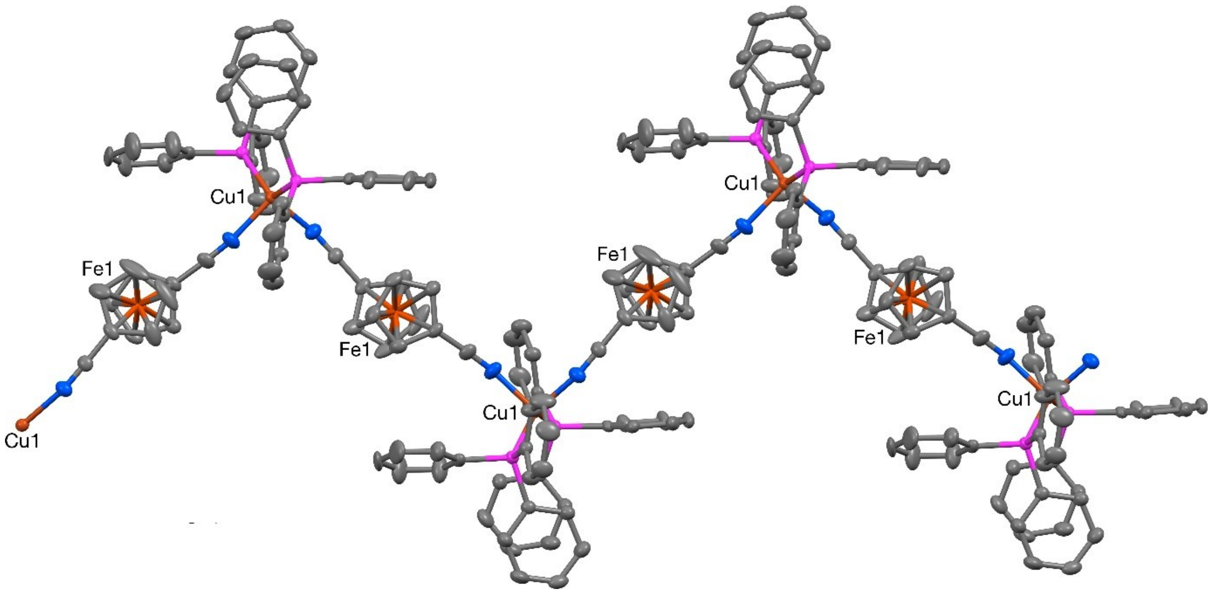

Figure S10: Part of the extended cationic polymer chain present in the structure of 5 (50% probability ellipsoids)..

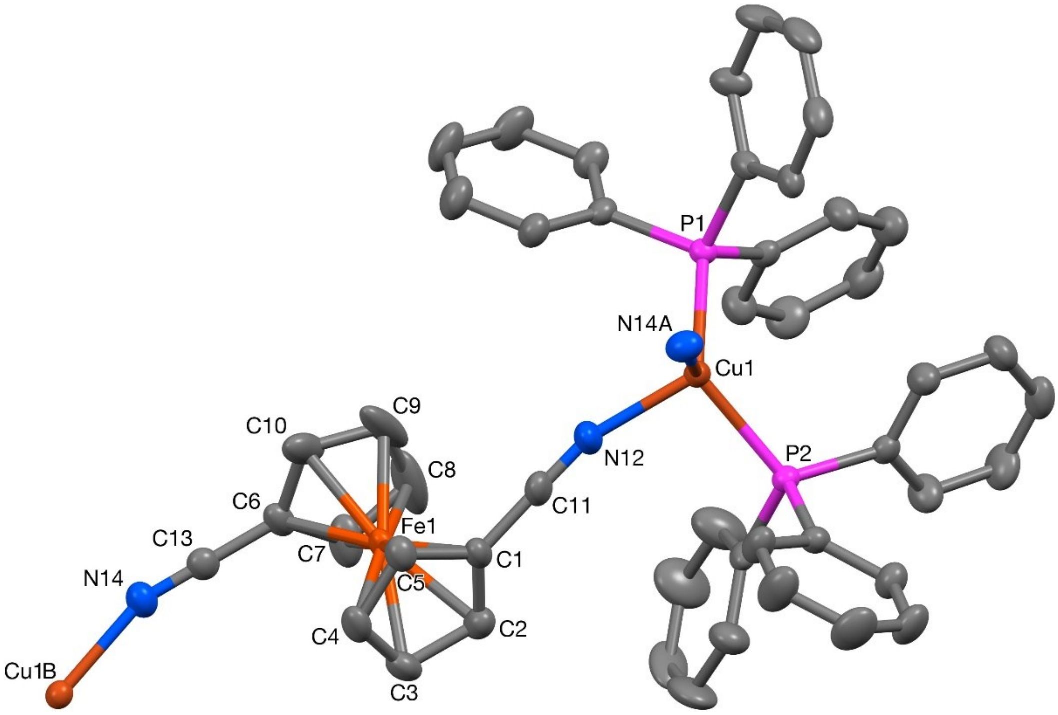

Figure S11: The structure of the unique portion of the cationic polymer chain present in the crystal of **5** showing how it links to adjacent atoms (50% probability ellipsoids).

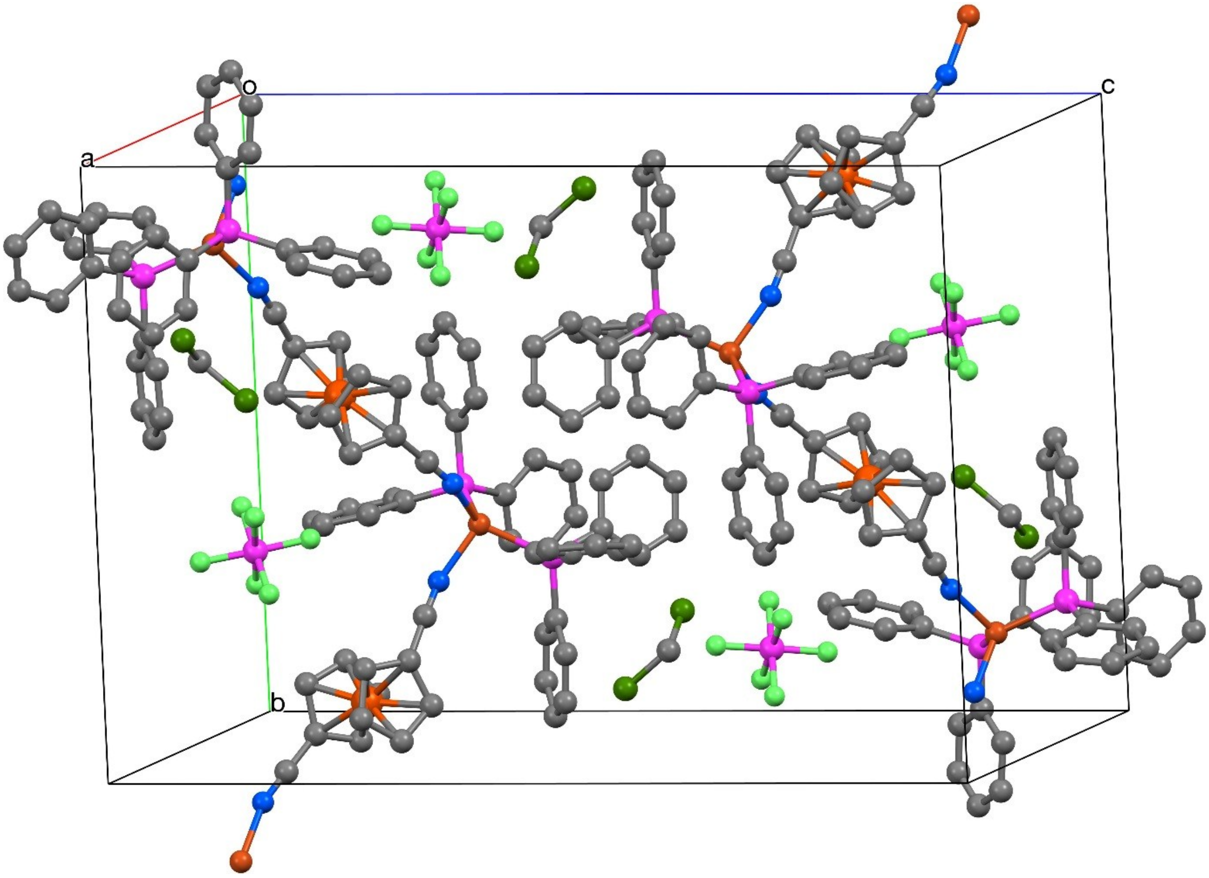

Figure S12: The contents of the unit cell in the structure of **5**.

Crystal data for **5**: [$C_{48}H_{38}CuFeN_2P_2$](PF_6)$_2$·CH_2Cl_2, *M* = 1054.03, monoclinic, $P2_1/n$ (no. 14), *a* = 11.0955(3), *b* = 17.6608(4), *c* = 24.8674(8) Å, β = 101.073(3)°, *V* = 4782.2(2) Å^3, *Z* = 4, D_c = 1.464 g cm^{-3}, μ(Mo-Kα) = 1.020 mm^{-1}, *T* = 173 K, orange blocks, Agilent Xcalibur 3 E diffractometer; 9568 independent measured reflections (R_{int} = 0.0227), F^2 refinement,[X1,X2] R_1(obs) = 0.0422, wR_2(all) = 0.1043, 7488 independent observed absorption-corrected reflections [$|F_o| > 4\sigma(|F_o|)$, completeness to θ_{full}(25.2°) = 98.6%], 632 parameters. CCDC 1873794.

The C45-based phenyl ring, the P60-based hexafluorophosphate anion, and the C70-based included dichloromethane solvent molecule in the structure of **5** were all found to be disordered. In each case two orientations were identified, of *ca*. 61:39, 86:14 and 79:21% occupancy respectively. The geometries of each pair of orientations were optimised, the thermal parameters of adjacent atoms were restrained to be similar, and only the non-hydrogen atoms of the major occupancy orientations were refined anisotropically (those of the minor occupancy orientations were refined isotropically).

Table S4. Selected bond lengths (Å) and angles (°) for **5**.

Cu(1)–P(1)	2.2536(7)	Cu(1)–P(2)	2.2662(8)
Cu(1)–N(12)	2.030(2)	Cu(1)–N(14A)	2.039(2)
C(11)–N(12)	1.142(4)	C(13)–N(14)	1.143(3)
P(1)–Cu(1)–P(2)	121.04(3)	P(1)–Cu(1)–N(12)	117.54(7)
P(1)–Cu(1)–N(14A)	106.13(7)	P(2)–Cu(1)–N(12)	99.36(7)
P(2)–Cu(1)–N(14A)	116.51(7)	N(12)–Cu(1)–N(14A)	93.12(10)

IR Spectroscopy

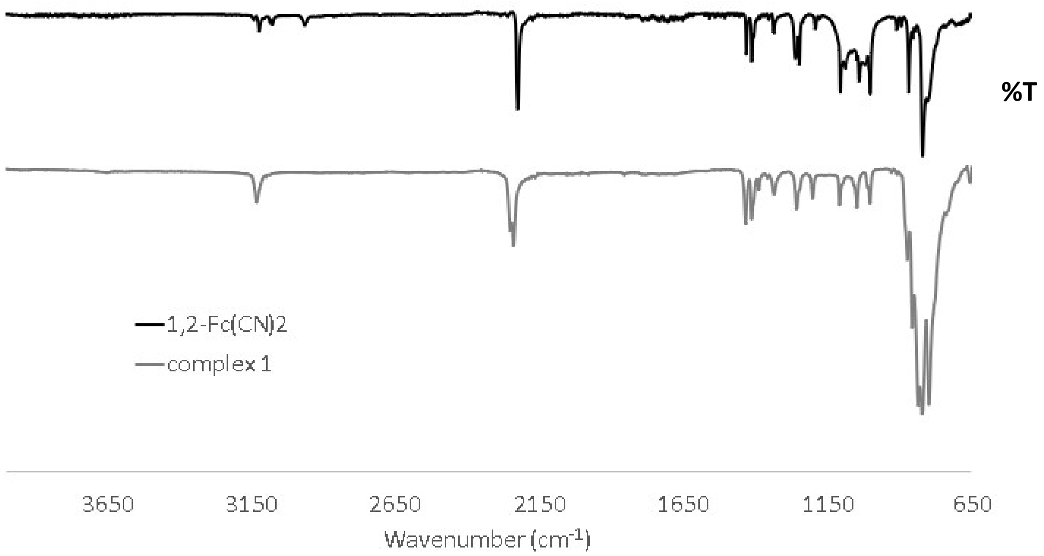

Figure S13: The solid state ATR-IR spectrum of 1,2-Fc($CN)_2$ (top, black) and complex **1** (bottom grey)

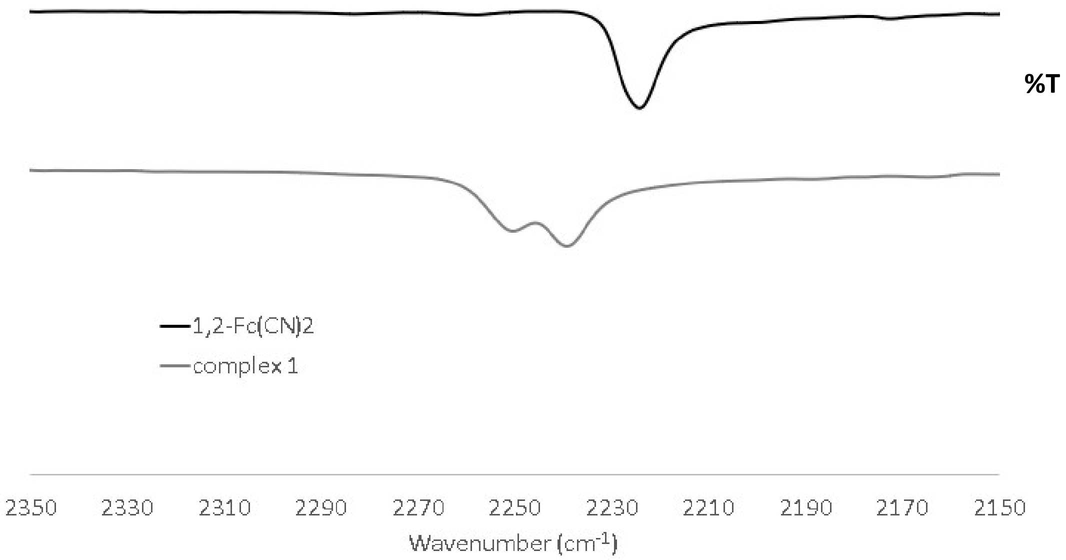

Figure S14: The *v*CN region of the solid state ATR-IR Spectrum of ligand 1,2-Fc($CN)_2$ (top, black) and complex **1** (bottom, grey)

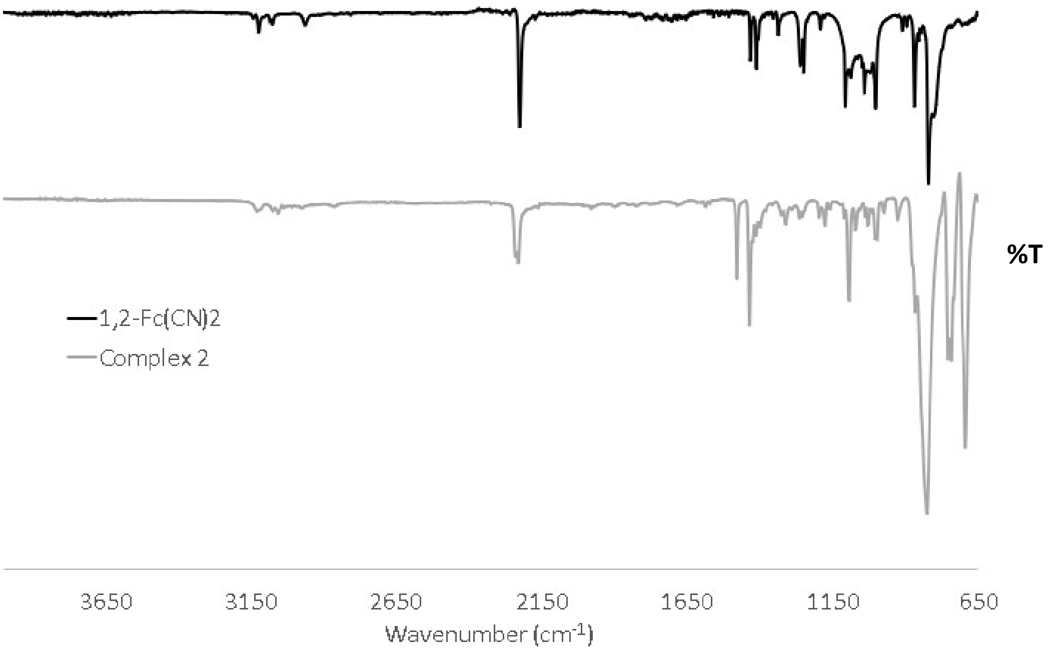

Figure S15: The solid state ATR-IR Spectrum of ligand 1,2-Fc(CN)$_2$ (top, black) and complex **2** (bottom, grey)

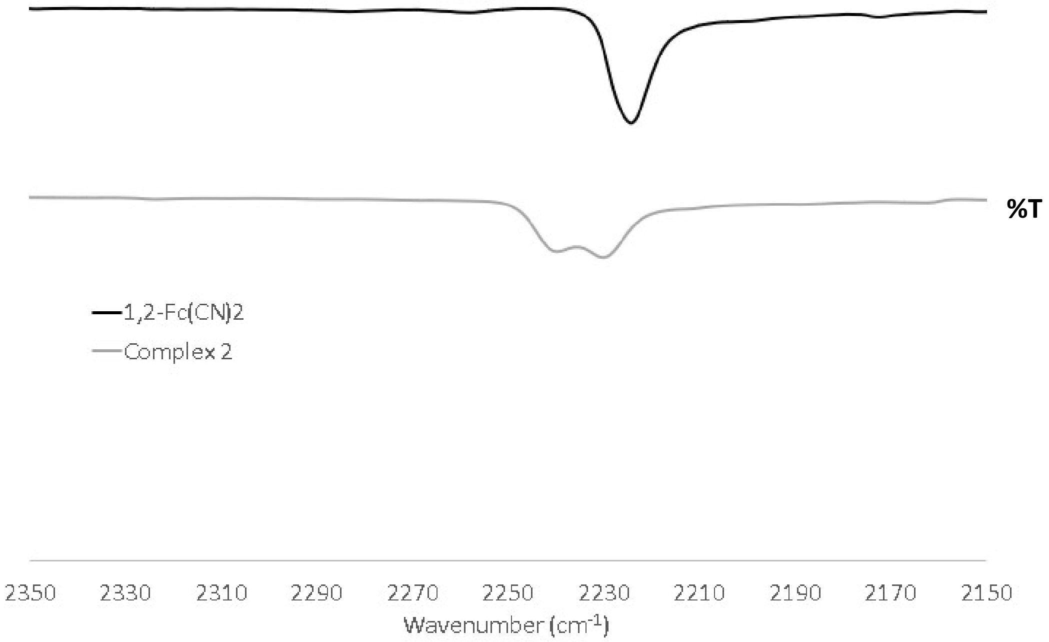

Figure S16: The *v*CN region of the solid state ATR-IR Spectrum of ligand 1,2-Fc(CN)$_2$ (top, black) and complex **2** (bottom, grey)

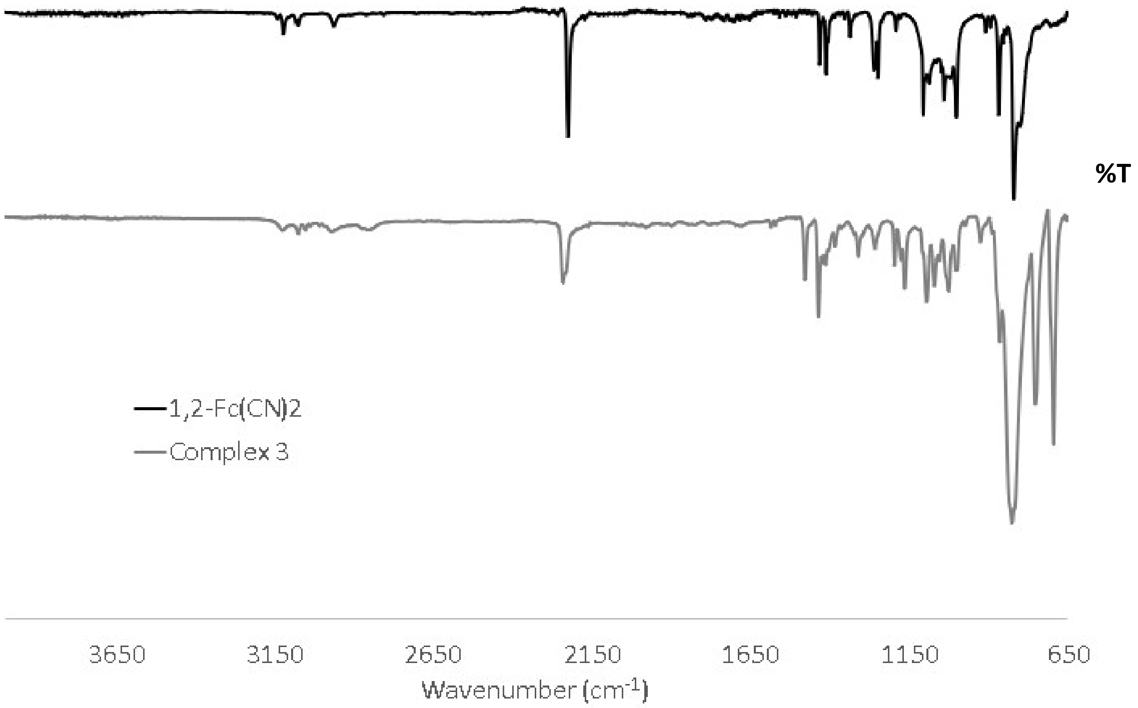

Figure S17: The solid state ATR-IR Spectrum of ligand 1,2-Fc(CN)$_2$ (top, black) and complex **3** (bottom, grey)

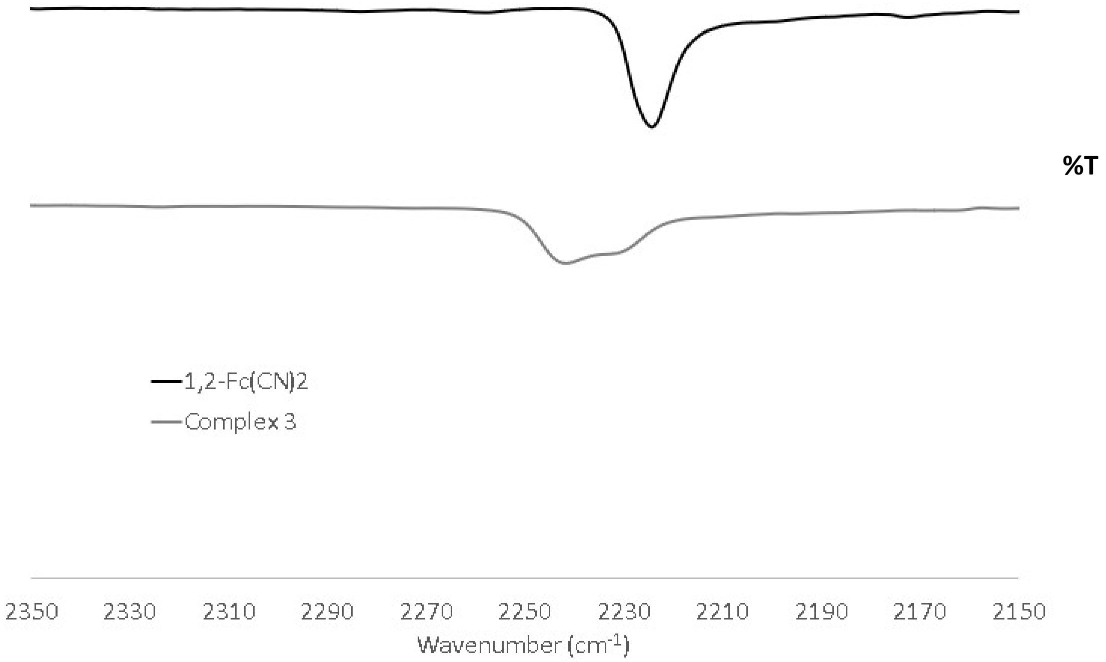

Figure S18: The *v*CN region of the solid state ATR-IR Spectrum of ligand 1,2-Fc(CN)$_2$ (top, black) and complex **3** (bottom, grey)

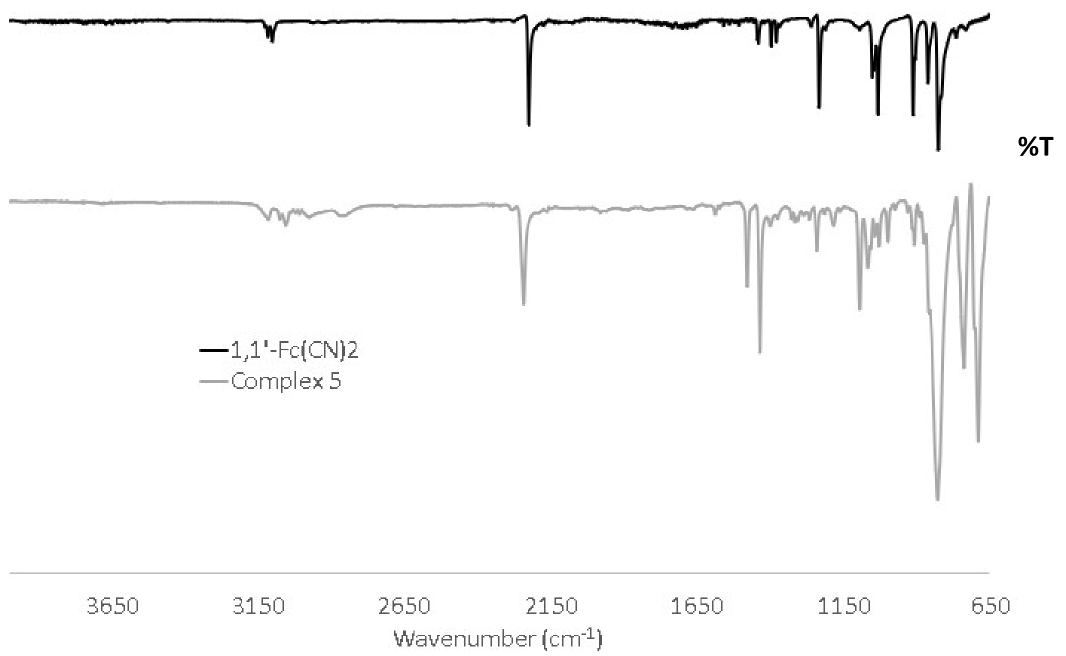

Figure S19: The solid state ATR-IR Spectrum of ligand 1,1'-Fc(CN)$_2$ (top, black) and complex **5** (bottom, grey)

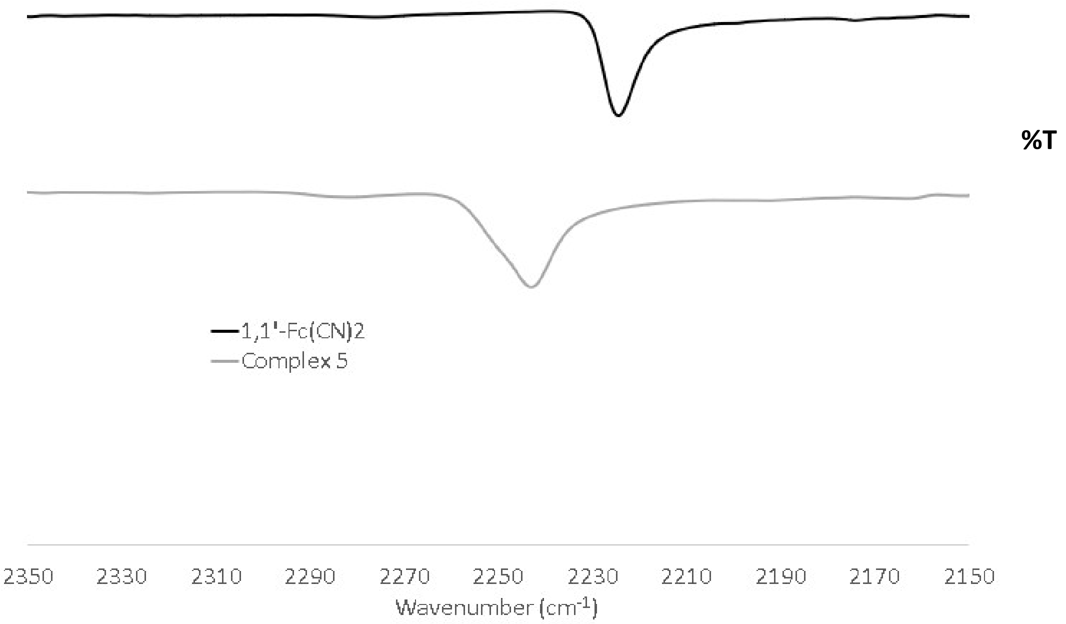

Figure S20: The *v*CN region of the solid state ATR-IR Spectrum of ligand 1,2-Fc(CN)$_2$ (top, black) and complex **5** (bottom, grey)

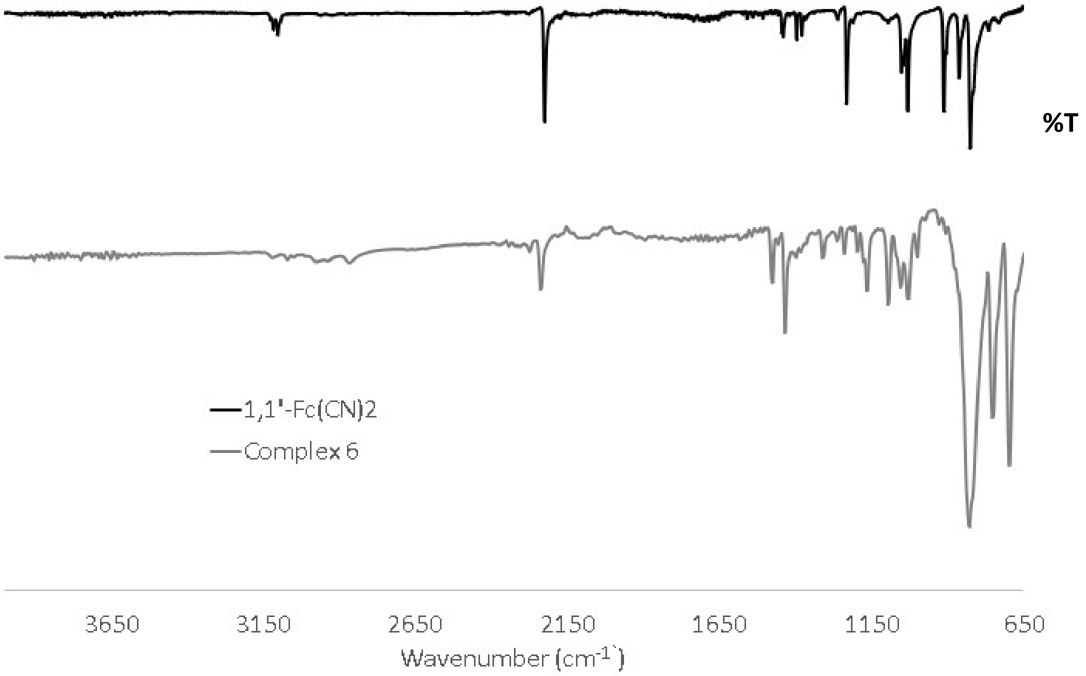

Figure S21: The solid state ATR-IR Spectrum of ligand 1,1′-Fc(CN)$_2$ (top, black) and complex **6** (bottom, grey)

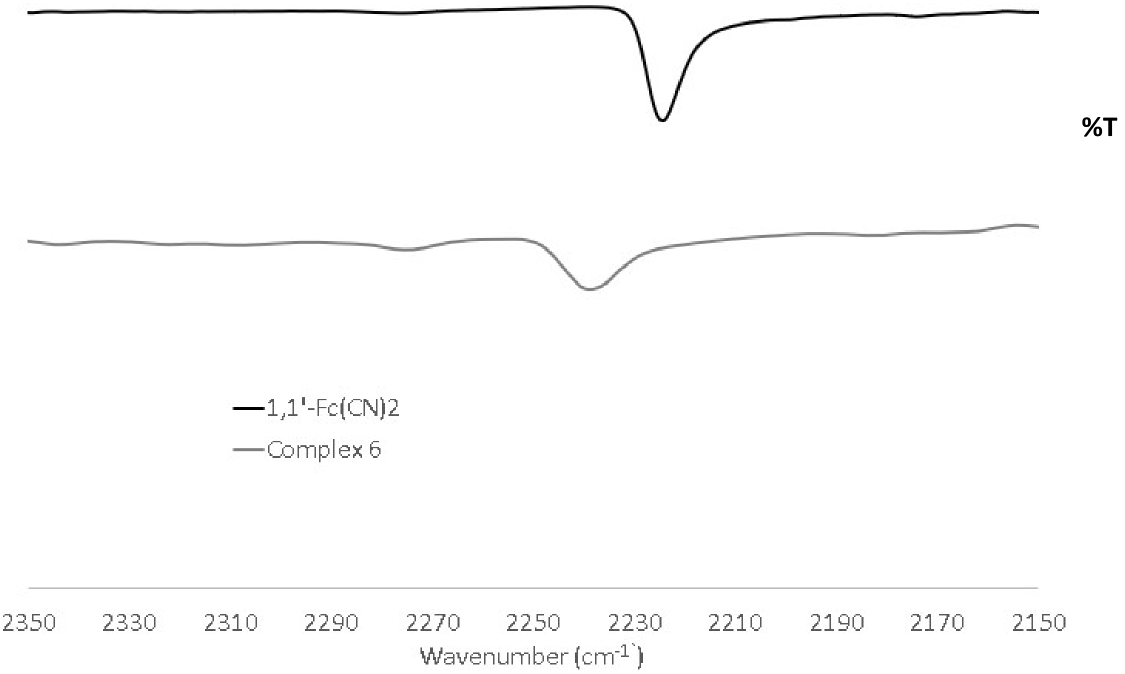

Figure S22: The *v*CN region of the solid state ATR-IR Spectrum of ligand 1,2-Fc(CN)$_2$ (top, black) and complex **6** (bottom, grey)

Lability studies

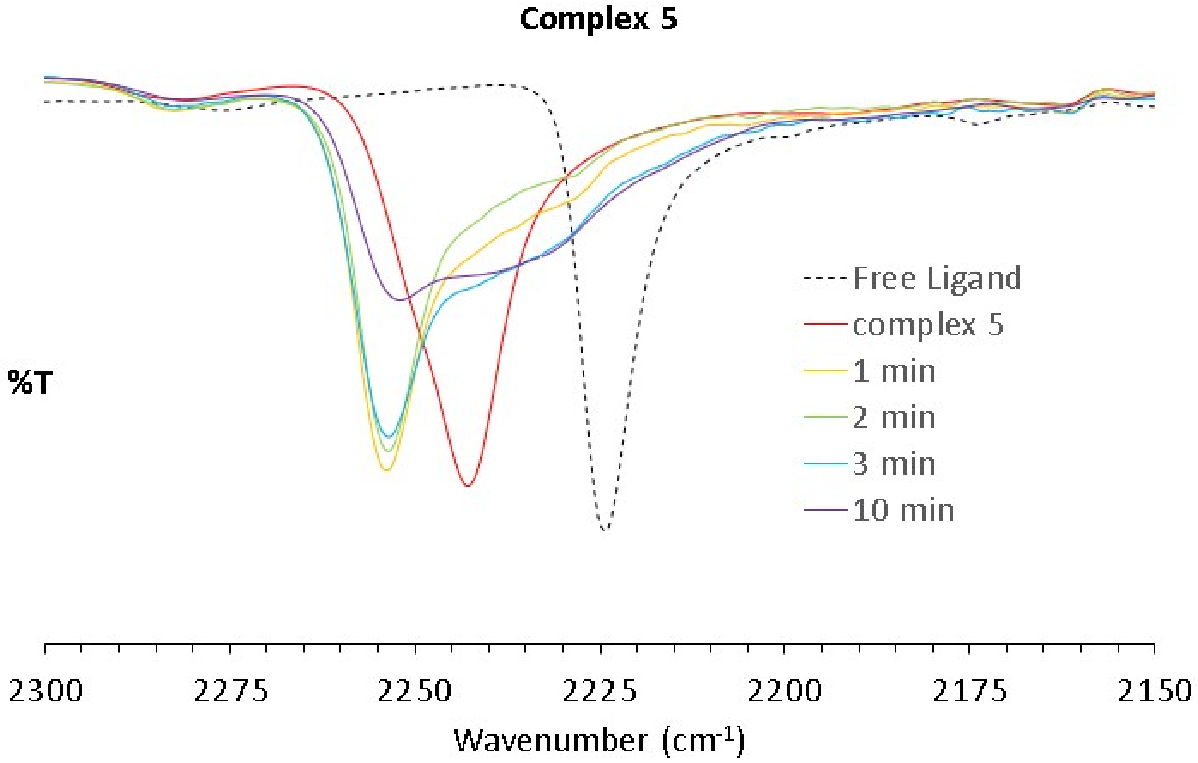

Figure S23: *v*CN region of the solid state ATR-IR spectrum of **5** displaying the variation in the signal with subsequent washes with acetone.

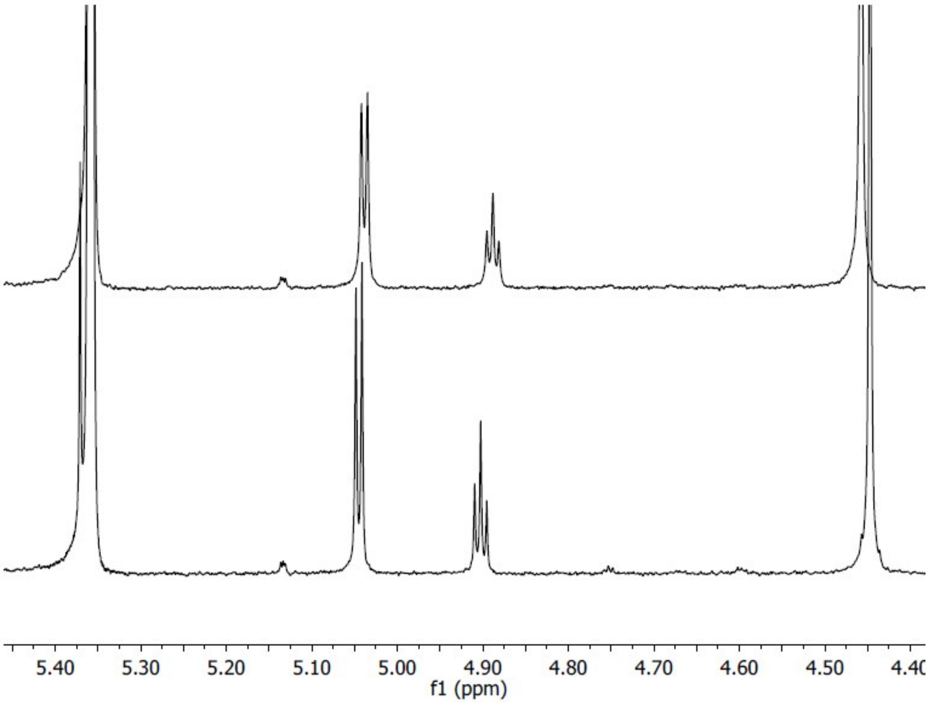

Figure S24: Cp region of the ^{1}H NMR spectrum (400 MHz) of **2** in CD_2Cl_2 taken before (top) and after the final IR trace (10 min in acetone)

Electrochemistry

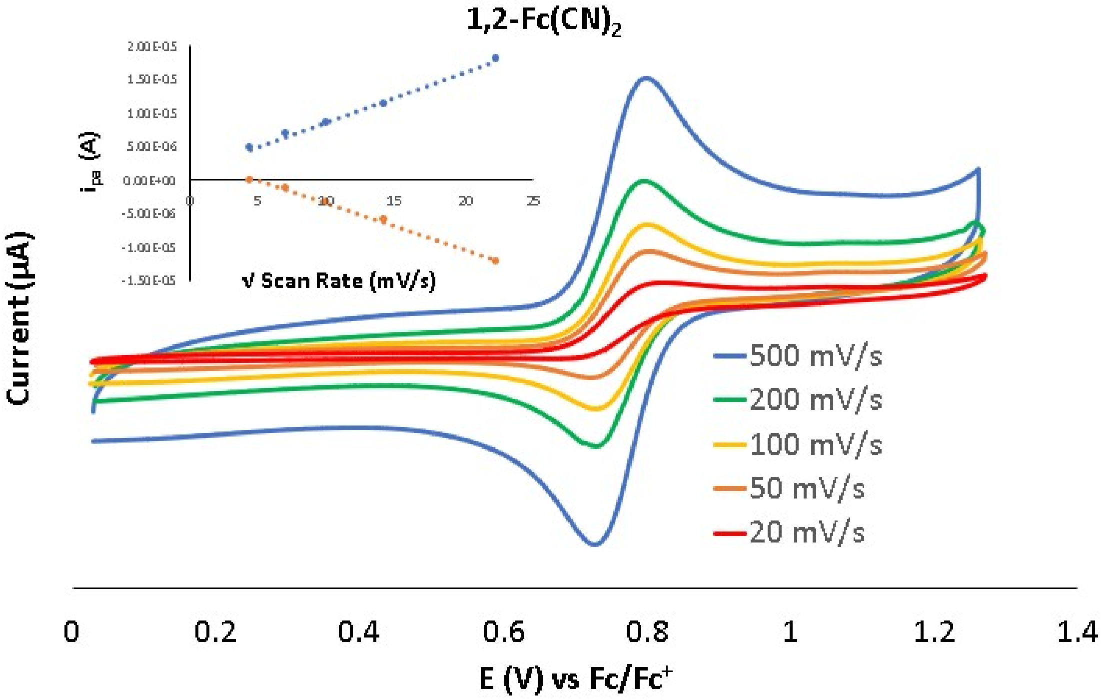

Figure S25: Cyclic voltammogram of 1,2-Fc(CN)$_2$ in 0.1 M N^{n}Bu$_4$PF$_6$ (CH$_2$Cl$_2$) at scan rates from 20-500 mV/s.

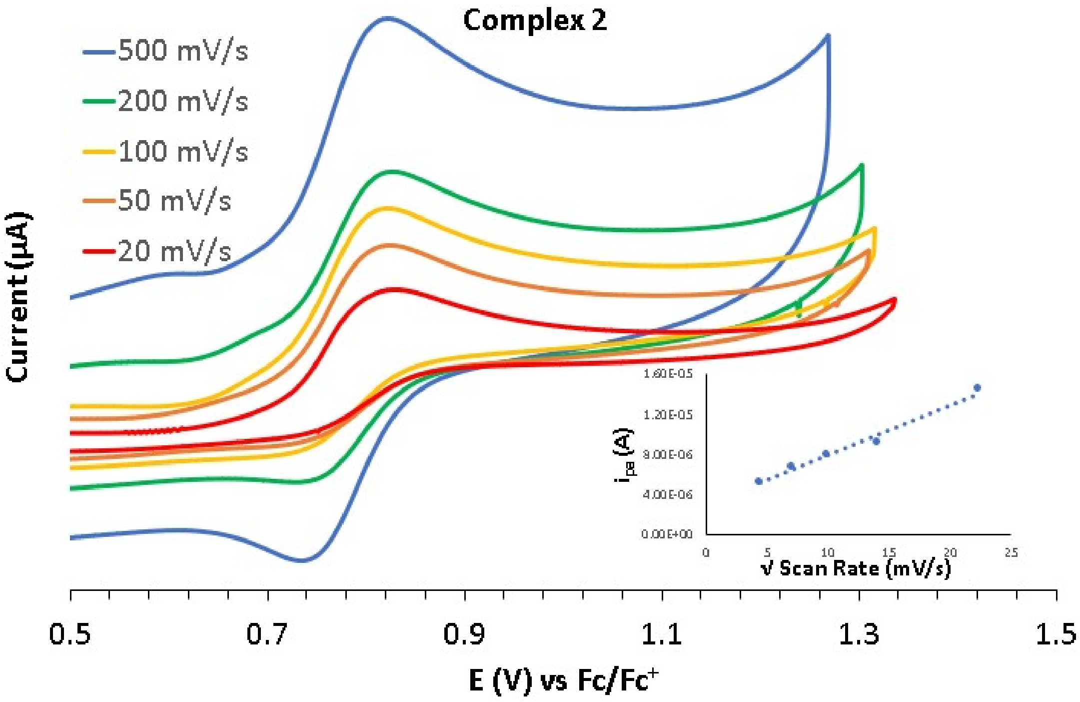

Figure S26: Cyclic voltammogram of complex **2** in 0.1 M N^{n}Bu$_4$PF$_6$ (CH$_2$Cl$_2$) at scan rates from 20-500 mV/s

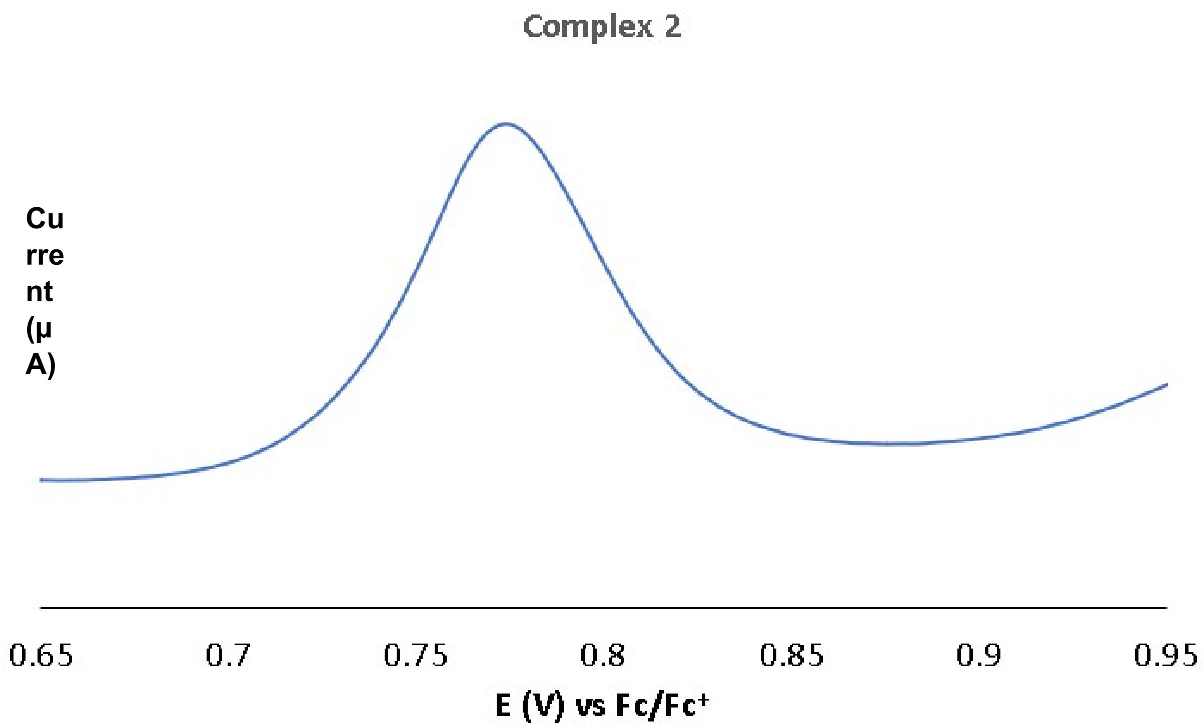

Figure S27: Differential pulse voltammogram of complex **2** in 0.1 M $N^nBu_4PF_6$ (CH_2Cl_2).

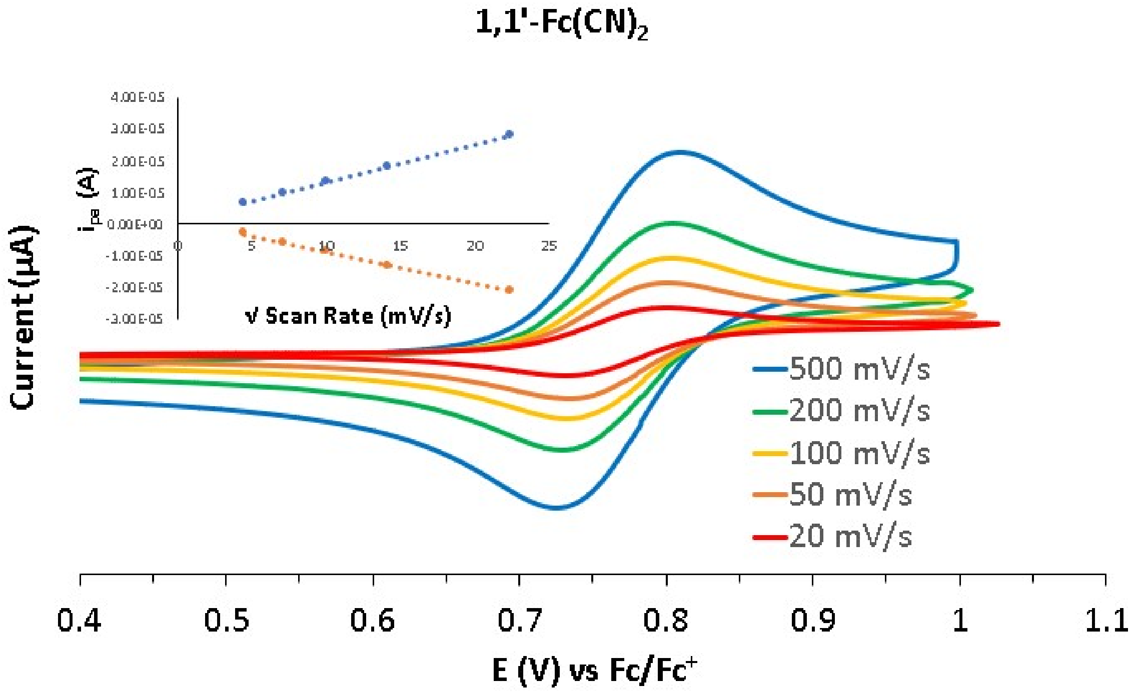

Figure S28: Cyclic voltammogram of 1,1’-$Fc(CN)_2$ in 0.1 M $N^nBu_4PF_6$ (CH_2Cl_2) at scan rates from 20-500 mV/s

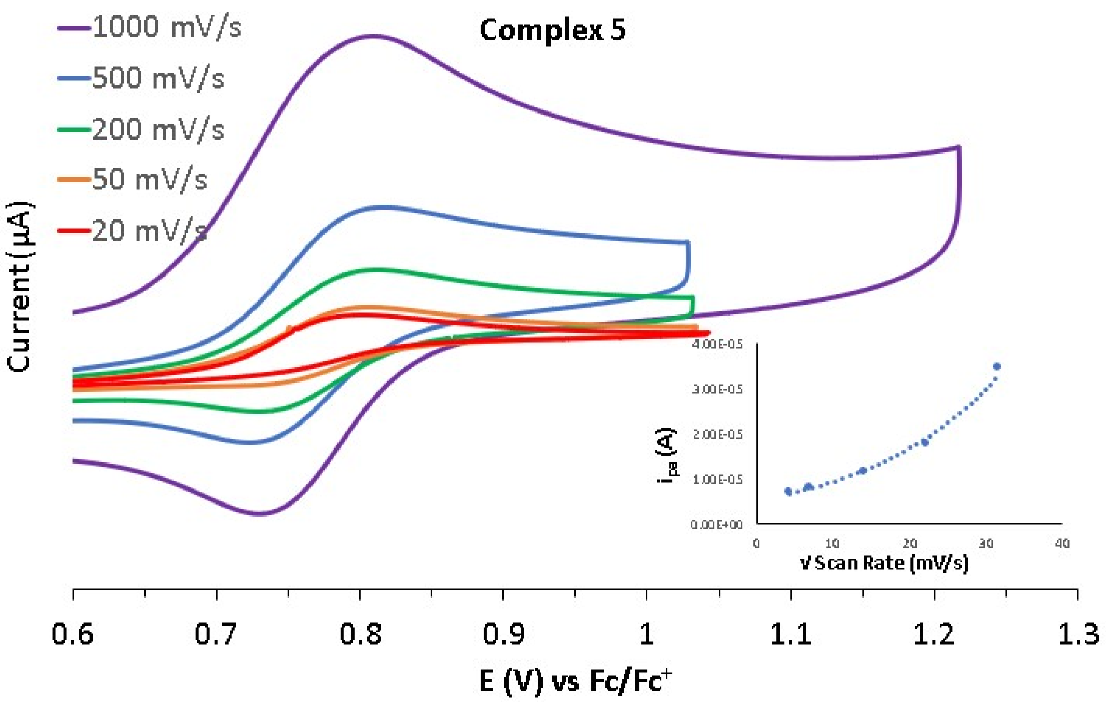

Figure S29: Cyclic voltammogram of complex **5** in 0.1 M N^{n}Bu$_4$PF$_6$ (CH$_2$Cl$_2$) at scan rates from 20-1000 mV/s

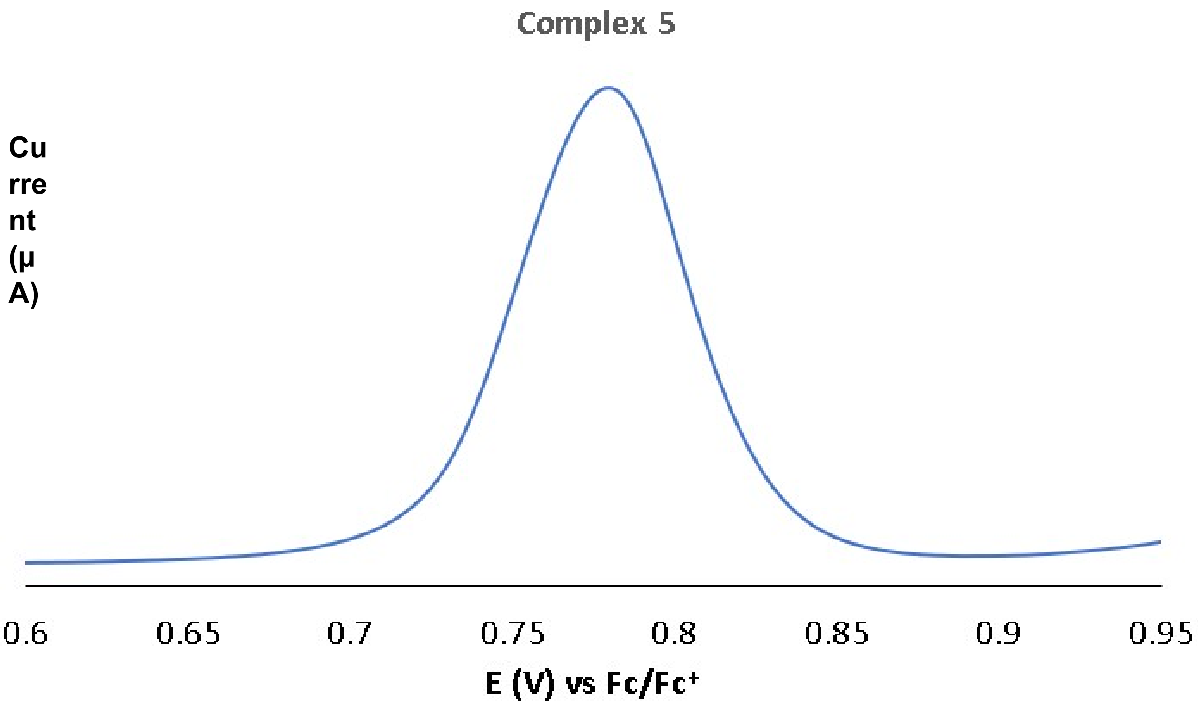

Figure S30: Differential pulse voltammogram of complex **5** in 0.1 M N^{n}Bu$_4$PF$_6$ (CH$_2$Cl$_2$).

References

[S1] G. J. Kubas, B Monzyk, A. L. Crumblis, *Inorg. Synth*, 1990, **28**, 68

[S2] G. G. A. Balavoine, G. Doisneau and T. Fillebeen-Kahn, *J. Organomet. Chem.*, 1991, **412**, 381–382.

[S3] E. G. Perevalova, L. P. Jureva and J. I. Baukov, *Dokl. Akad. Nauk SSSR*, 1968, **135**, 1402.

[S4] W. Steffen, M. Laskoski, G. Collins and U. H. F. Bunz, *J. Organomet. Chem.*, 2001, **630**, 132–138.

[X1] SHELXTL v5.1, Bruker AXS, Madison, WI, 1998.

[X2] SHELX-2013, G.M. Sheldrick, *Acta Cryst.*, 2015, **C71**, 3-8.